



St. Paul Island, Pribilof Islands, Alaska : geology, volcanic evolution, and volcanic hazards
by Grace Sherwood Winer

A thesis submitted in partial fulfillment of the requirements for the degree of Master of Science in
Earth Sciences

Montana State University

© Copyright by Grace Sherwood Winer (2001)

Abstract:

St. Paul Island, Alaska, is a potentially active Pleistocene to Holocene volcanic center located in the Bering Sea about 400 km north of the Aleutian arc front. Previous geological mapping and studies of the geology of St. Paul Island have been done only in reconnaissance. This study has been undertaken in order to make the first detailed geological map of the island, to reconstruct its eruptive history and volcanic evolution, and to assess volcanic hazards that may be associated with future eruptions. New geological mapping covers the entire island at a scale of 1:28,000 and includes 17 volcanic units. Eruptive styles on St. Paul have evolved from early, mostly effusive eruptions of primitive lavas that form the platform of the island, to more explosive monogenetic cinder cones emplaced upon the platform, to the polygenetic centers that are forming large shields from repeated eruptions of evolved low viscosity lavas. Lavas erupted are mainly basalts, basanites, and tephrites with MgO contents ranging from 14 to 4 wt% and phenocryst assemblages of olivine \pm clinopyroxene and plagioclase. St. Paul's volcanic system as a whole is trending toward the progressive development of shallow crustal magma chambers where cooling and differentiation are occurring. A new ^{14}C date of 3230 ybp has been obtained on the youngest lava flow on St. Paul. Volcanic hazards associated with a future eruption on St. Paul Island are similar to those from dominantly Strombolian style eruptions at other basaltic lava fields. However, because of St. Paul's unique human and wildlife populations, isolated location, and extreme weather conditions in the Bering Sea, volcanic risks may be exacerbated. Assuming a predictable eruption recurrence interval of 7400 years, the probability of an eruption on St Paul Island in future decades is estimated to be extremely small.

ST. PAUL ISLAND, PRIBILOF ISLANDS, ALASKA:
GEOLOGY, VOLCANIC EVOLUTION, AND VOLCANIC HAZARDS

by

Grace Sherwood Winer

A thesis submitted in partial fulfillment
of the requirements for the degree

of

Master of Science

in

Earth Sciences

MONTANA STATE UNIVERSITY
Bozeman, Montana

April 2001

© COPYRIGHT

by

Grace Sherwood Winer

2001

All Rights Reserved

N378
W7255

APPROVAL

of a thesis submitted by

Grace Sherwood Winer

This thesis has been read by each member of the thesis committee and has been found to be satisfactory regarding content, English usage, format, citations, bibliographic style, and consistency, and is ready for submission to the College of Graduate Studies.

Todd C. Feeley

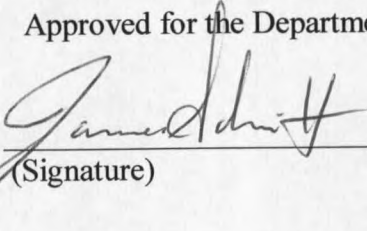


(Signature)

4-12-01
Date

Approved for the Department of Earth Sciences

James G. Schmitt

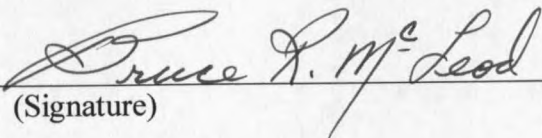


(Signature)

4-12-01
Date

Approved for the College of Graduate Studies

Bruce McLeod



(Signature)

4-13-01
Date

STATEMENT OF PERMISSION TO USE

In presenting this thesis in partial fulfillment of the requirements for a master's degree at Montana State University, I agree that the Library shall make it available to borrowers under the rules of the Library.

If I have indicated my intention to copyright this thesis by including a copyright notice page, copying is allowable only for scholarly purposes, consistent with "fair use" as prescribed in the U.S. Copyright Law. Requests for permission for extended quotation from or reproduction of this thesis in whole or in parts may be granted only by the copyright holder.

Signature



Date

APRIL 17, 2001

ACKNOWLEDGEMENTS

Support for this project was generously provided by the National Geographic Society, the Geological Society of America, and Sigma Xi Grants-in-Aid of Research. I am indebted to the people of St. Paul Island for their warm hospitality and assistance, without which our work on St. Paul would have been very difficult indeed. Thank you Phyllis Swetzof, Aquilina Bourdukofsky, Karin Holser, and so many others. Special thanks to Dr. David Lageson for introducing me to the fascinating field of geology and for advice, support and encouragement throughout my undergraduate and graduate years at Montana State University. Thanks to Dr. George Plafker and Dr. Ken Pierce for consultation on Bering Sea tectonics; to Dr. Mel Kuntz for advice on organic carbon sampling; and to Dr. Joseph Ashley for advice on interpretation of aerial photographs and map technicalities. Special thanks to Anne Loi for technical support and encouragement. Thanks to Dr. J.J. Borkowski for consultation on statistics, to the staff at the NOAA National Weather Service station on St. Paul Island for data on weather and tides, and to Peter Gauer for interpretation of weather data. Thanks to my committee members, Dr. Jim Schmitt and Dr. Bill Locke, for their insight and helpful suggestions. My deepest gratitude to my advisor Dr. Todd Feeley for years of patience, helpful discussions, guidance, and advice, both in the field and at MSU. I thank Bernie for unwavering support over the years, my family for their encouragement and confidence in me, and Ruth for introducing me to St. Paul Island.

TABLE OF CONTENTS

1. INTRODUCTION.....	1
Statement of Purpose	1
Geographic Location and Description of St. Paul Island	2
Regional Geology and Tectonic Setting.....	4
Geology of St. Paul Island: Previous Work and Current State of Knowledge.....	7
2. METHODS	16
Mapping and Sample Collection.....	16
X-ray Fluorescence	17
Petrography.....	17
Geochronology.....	18
3. GEOLOGY OF ST. PAUL ISLAND	19
Ages of Rocks on St. Paul Island.....	19
Classification and Composition of St. Paul Rocks	20
Geological Map of St. Paul Island	34
Descriptions and Interpretations of Map Units.....	36
Undifferentiated Platform Lavas (UPL) Description	36
Kaminista Description	46
Kaminista Interpretation	48
Undifferentiated Platform Lavas (UPL) Interpretation	50
Undifferentiated Lava Flows (ULF) Description.....	52
Undifferentiated Lava Flows (ULF) Interpretation	52
PyC Unit Description.....	52
PyC Unit Interpretation.....	55
Black Bluffs (BB) Description.....	56
Black Bluffs (BB) Interpretation.....	58
Polovina Hill (POL) Description.....	60
Polovina Hill (POL) Interpretation.....	64
Hill 404 (404) Description	66
Hill 404 (404) Interpretation	67
North Hill (NoH) Description	67
North Hill (NoH) Interpretation	69
Hill 255 (H255) Description	69
Hill 255 (H255) Interpretation	70
Crater Hill (CH) Description.....	71
Crater Hill (CH) Interpretation.....	73

TABLE OF CONTENTS - CONTINUED

Lake Hill (LH) Description.....	74
Lake Hill (LH) Interpretation.....	77
Ridge Hill (RiH) Description.....	77
Ridge Hill (RiH) Interpretation.....	78
Rush Hill (RuH) Description.....	79
Rush Hill (RuH) Interpretation.....	81
Ridge Wall (RW) Description.....	82
Ridge Wall (RW) Interpretation.....	85
Hutchinson Hill (HH) and Northeast Point Description.....	86
Hutchinson Hill (HH) Interpretation.....	88
Airport Lava Field (ALF) Description.....	89
Airport Lava Field (ALF) Interpretation.....	90
Cone Hill Volcanic Complex (CHVC) Description.....	91
Cone Hill Volcanic Complex (CHVC) Interpretation.....	95
Bogoslof Hill Volcanic Complex (BHVC) Description.....	100
Bogoslof Hill Volcanic Complex (BHVC) Interpretation.....	106
Fox Hill (FXH) Description.....	109
Fox Hill (FXH) Interpretation.....	114
Surficial Deposits (Sd) Description.....	115
Faulting and Fissuring.....	116
Volcanic and Structural Lineaments.....	119
Xenoliths in St. Paul Lavas.....	124
4. SUMMARY.....	126
Volcanic Evolution of St. Paul Island.....	126
Platform Building Stage.....	126
Monogenetic Cinder Cone Stage.....	128
Polygenetic Shield Stage.....	133
Compositional and Petrologic Evolution of St. Paul Island.....	136
5. POTENTIAL VOLCANIC HAZARDS AND RELATED RISKS.....	140
Introduction and Definitions.....	140
Hazard Assessment.....	142
Potential Volcanic Hazards.....	143
Estimate of Eruptive Intervals and Prediction.....	144
Volcanic Hazard Characteristics and Associated Risks on St. Paul Island.....	146
Lava Flows.....	146

TABLE OF CONTENTS - CONTINUED

Tephra Falls.....	147
Ballistic Ejecta.....	148
Volcanic Gases.....	149
Ground Deformation.....	149
Earthquakes: Seismicity of Volcanic Origin.....	149
Tsunami.....	150
Base Surge.....	150
Factors That May Exacerbate Risks on St. Paul Island.....	151
Hazard Mapping.....	152
Suggestions for Dealing with Future Volcanic Eruptions.....	154
6. CONCLUSIONS.....	156
REFERENCES CITED.....	158
APPENDIX A: RADIOCARBON SAMPLE PREPARATION AND ANALYTICAL TECHNIQUES.....	168

LIST OF TABLES

Table

1. Major Element, Trace Element, and Modal Analyses of Volcanic Rocks and Xenoliths from St. Paul Island, Alaska	22
2. CIPW Calculated Normative Minerals in Weight Percent and Rock Names	29

LIST OF FIGURES

Figures

1. Location of St. Paul Island	3
2. Tectonic setting of St. Paul Island.....	5
3. Barth's geologic map of St. Paul Island	9
4. Classification of the rocks	21
5. Pahoehoe flow lobe details	37
6. Lava tube near sea level at Southwest Point.....	38
7. Lava toes and columnar jointing in lava flow lobes at Reef Point	39
8. Marine and beach sediments at Tolstoi Point	40
9. Lava flows at Tolstoi Point thicken upward	40
10. Schematic diagram of stratigraphy at Zapadni Point	41
11. Schematic diagram of vertical section at Einahnuhto Bluffs on St. Paul's west coast	43
12. Photomicrographs showing textures of platform lavas	45
13. Kaminista ridge with view to the northeast	47
14. Kaminista.....	49
15. Black Bluffs, the emergent tuff/cinder cone located near the village of St. Paul	57
16. Close-up view of Black Bluffs.....	57
17. Diagram of Surtseyan eruption at Black Bluffs	59

LIST OF FIGURES - CONTINUED

18. Polovina Hill, a large complex cinder cone, dominates eastern St. Paul Island.....	60
19. Vertical section on east flank of Polovina Hill is exposed in a quarry	61
20. Bombs from Polovina Hill.....	62
21. Photomicrograph of trachyte from Polovina Hill (SP98-35).....	63
22. North Hill is a complex cinder cone located on northern St. Paul Island.....	68
23. Olivine-rich North Hill basanite with glassy groundmass.....	68
24. Crater Hill viewed across a lava flow from Bogoslof Hill.....	72
25. Photomicrograph of lherzolite xenolith (left) in Crater Hill lava (SP98-50)	73
26. At Lake Hill, vents are located on intersecting NE-SW lineaments.....	76
27. Schematic diagram of Ridge Hill cinder cone and proposed mechanism for basal cone spreading (Kuntz et al., 1982).....	79
28. Schematic diagram of section through Rush Hill and Einahnuhto Bluffs on the west coast of St. Paul Island (Barth, 1956).....	80
29. Praying Aleut	84
30. Photomicrograph of Ridge Wall olivine basalt (SP98-42).....	84
31..Photomicrograph of granitoid xenolith (left and upper right) in Ridge Wall lava (SP98-43X).....	85
32. Hutchinson Hill located on Northeast Point	87

LIST OF FIGURES – CONTINUED

33. Photomicrograph of crystal-rich Hutchinson Hill basalt (SP98-04).....	88
34. View from Kittiwake Lake caldera looking northeast along the Cone Hill ridge	92
35. Fissure on Cone Hill ridge.....	93
36. Exposure of feeder dike in Cone Hill ridge.....	93
37. Collapsed lava tube on southwestern Cone Hill ridge	94
38. Photomicrograph of glomeroporphyritic CHVC lavas	95
39. Proposed mechanism for formation of lava dome in Cone Hill volcanic complex.....	99
40. Profile of Bogoslof Hill as seen from Lake Hill	100
41. Northwest cone on Bogoslof Hill.....	101
42. Fissure in lava tongue on east flank of Bogoslof Hill strikes E-W across Bogoslof summit	103
43. Photomicrographs of BHVC lavas.....	105
44. Fox Hill cinder cone and lava flow (FXH).....	110
45. Sample site for ^{14}C in layer of sediment beneath Fox Hill lava flow (SP98-64)	111
46. Segments of the breached Fox Hill cinder cone that have been rafted along on the Fox Hill lava flow	111
47. Fox Hill lava flow at Southwest Point.....	112
48. Photomicrograph of fractionated Fox Hill lava	113
49. Faulting of platform lavas on Tolstoi Point.....	117

LIST OF FIGURES - CONTINUED

50. Fissure on Bogoslof Hill.....	118
51. Volcanic and structural lineaments on St. Paul Island and surrounding area.....	120
52. Lineaments of volcanic vents, fissures, and faults on St. Paul Island.....	121
53. Rose diagrams showing directional trends of A: fissures, B: cone breaching, C: faults, and D: vent alignments.....	123
54. Platform lavas on the west coast.....	127
55. Schematic diagram of a monogenetic volcanic field.....	129
56. Relationship of Village Hill cinder cone to platform lavas.....	131
57. Remnant of scoria cone on lava flows on east Reef Point.....	132
58. Schematic diagram of coalescing dikes forming a shallow magma chamber beneath Bogoslof Hill.....	135
59. Variation diagrams showing increasing evolution and fractionation of lavas from platform to monogenetic to polygenetic centers.....	137
60. Area of possible future lava flows from Bogoslof Hill volcano.....	153

LIST OF PLATES

Plates

1. Geological Map of St. Paul Island, Alaska..... Pocket
2. Cone Hill Volcanic Complex (CHVC) Pocket

ABSTRACT

St. Paul Island, Alaska, is a potentially active Pleistocene to Holocene volcanic center located in the Bering Sea about 400 km north of the Aleutian arc front. Previous geological mapping and studies of the geology of St. Paul Island have been done only in reconnaissance. This study has been undertaken in order to make the first detailed geological map of the island, to reconstruct its eruptive history and volcanic evolution, and to assess volcanic hazards that may be associated with future eruptions. New geological mapping covers the entire island at a scale of 1:28,000 and includes 17 volcanic units. Eruptive styles on St. Paul have evolved from early, mostly effusive eruptions of primitive lavas that form the platform of the island, to more explosive monogenetic cinder cones emplaced upon the platform, to the polygenetic centers that are forming large shields from repeated eruptions of evolved low viscosity lavas. Lavas erupted are mainly basalts, basanites, and tephrites with MgO contents ranging from 14 to 4 wt% and phenocryst assemblages of olivine \pm clinopyroxene and plagioclase. St. Paul's volcanic system as a whole is trending toward the progressive development of shallow crustal magma chambers where cooling and differentiation are occurring. A new ^{14}C date of 3230 ybp has been obtained on the youngest lava flow on St. Paul. Volcanic hazards associated with a future eruption on St. Paul Island are similar to those from dominantly Strombolian style eruptions at other basaltic lava fields. However, because of St. Paul's unique human and wildlife populations, isolated location, and extreme weather conditions in the Bering Sea, volcanic risks may be exacerbated. Assuming a predictable eruption recurrence interval of 7400 years, the probability of an eruption on St Paul Island in future decades is estimated to be extremely small.

INTRODUCTION

Statement of Purpose

Previous studies of the volcanic geology, including petrology and petrography, of St. Paul Island have been done mostly in reconnaissance (Stanley-Brown, 1892; Barth, 1956; Cox et al., 1966; Hopkins, 1976; Lee-Wong et al., 1979; Moll-Stalcup, 1994a, 1994b). Past workers have not made a detailed investigation of the eruptive history of the island correlated with changes in magma composition, nor have they presented any studies related to volcanic hazards in the event of a future eruption. However, they have suggested that volcanic eruptions on St. Paul have been a regular occurrence for about the last 300-400 Ka with eruptions taking place within the last 10,000 years, and the most recent occurring only a few thousand years ago (Cox et al., 1966; Hopkins, 1976). Cox et al. (1966) and Hopkins (1976) agree that future volcanic eruptions on St. Paul Island are to be expected. Therefore, this field study of the volcanic geology of St. Paul Island and investigation of petrography and compositional trends of St. Paul magmas is undertaken for the purpose of: (1) increasing knowledge of the stratigraphy of St. Paul Island by field mapping and use of petrography and geochemistry to correlate eruptive units, (2) documenting the age and character of (a) the layered lava flows that form the platform of the island and (b) the morphologically younger units on the island's surface, (3) describing and interpreting the volcanic geology of St. Paul Island, especially the most recent volcanism, and (4) using 1-3 to make a general prediction of possible future

eruptions, their probable locations and styles, and to make an assessment of associated volcanic hazards on St. Paul Island. This work builds upon previous studies of St. Paul by Winer and Feeley (1997) and Feeley and Winer (1999), which show evidence for the development of shallow crustal magma chambers beneath the island.

The volcanic hazard assessment at St. Paul island is not only relevant because of its human inhabitants, but also because St. Paul is the seasonal breeding ground for nearly a million northern fur seals [the world's largest herd of marine mammals (Johnson, 1982)], the nesting site for large colonies of seabirds, home to a herd of several hundred reindeer, and port for the Central Bering Sea fishing fleet. Because of its rich wildlife, St. Paul Island, in spite of its remote location, is also an international tourism destination.

Geographic Location and Description of St. Paul Island

St. Paul Island is located in the Bering Sea about 440 km north of the Aleutian Island chain and 500 km west of the Alaska mainland at approximately 57° 07' N Latitude, 170° 16' W Longitude (Fig. 1). St. Paul is situated on the southern edge of the shallow and extensive Bering Sea shelf, near the 180 m depth contour, which represents a sharp break in bottom topography between the shelf and the abyssal Bering Sea (Fig. 1). St. Paul Island is the largest (40.4 mi²; 104 km²) of the Pribilof Islands, which consist of St. Paul and St. George, the two largest islands, and three islets located near St. Paul. The islets are Otter Island, about 1 km in length, and two smaller rocky outcrops, Sea Lion Rock and Walrus Island, over which the sea breaks in stormy weather. St. George and St. Paul,

the only inhabited islands, are each about 20 km long and are separated by 70 km. They have an arctic marine climate and the area is infamous for fog and inclement weather.

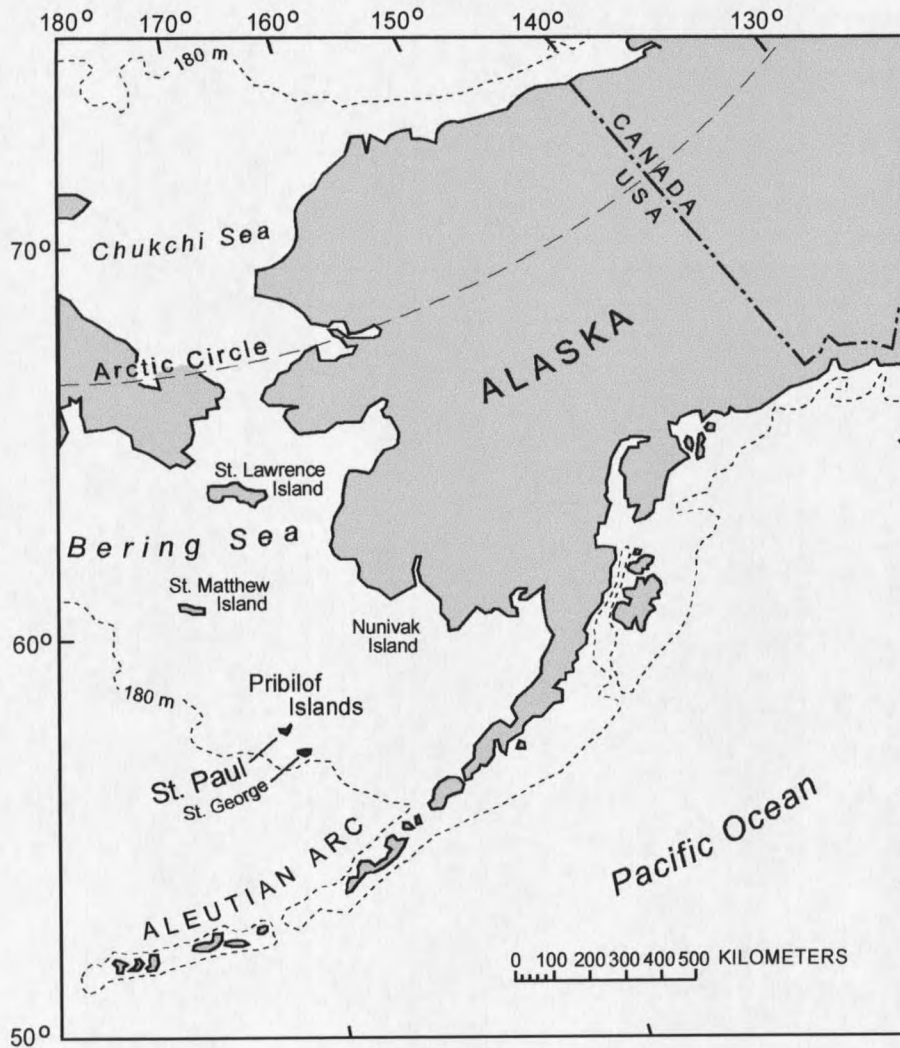


Figure 1. Location of St. Paul Island. Index map showing St. Paul Island, the Pribilof Islands, and their location on the southern edge of the Bering sea shelf. The approximate position of the shelf edge is marked by the dashed 180 m depth contour.

The Pribilof Islands, the hauling grounds for the great herds of northern fur seals, were uninhabited by humans until 1786, when they were discovered by the Russian mariner, Gehrman Pribylov (Elliott, 1881). Soon after their discovery, the Russians brought a number of Aleut people from the Aleutian Islands to the Pribilof Islands for the purpose of harvesting seal furs (Johnson, 1982). Descendents of these early settlers live on St. Paul today in the largest Aleut community (population ~750) in the world and the center of Aleut culture.

Scientific studies of the Pribilof Islands, also known as the Seal Islands, began soon after the United States acquired the territory of Alaska in 1867. Because St. Paul is the main breeding ground of the great fur seal herds, this small, remote island was the focus of many early studies, not only in geology, but also in zoology, botany, and paleontology (Hanna, 1919).

Regional Geology and Tectonic Setting

St. Paul Island is a locus of young and persistent basaltic volcanism situated in the Bering Sea about 440 km north of the Aleutian arc front. St. Paul Island, and the other Pribilof Islands, are constructed of basaltic lavas extruded onto the Pribilof Ridge, a northwest trending structural arch on the southern Bering Sea shelf (Marlow et al., 1976; Marlow et al., 1994) (Fig. 2). Volcanic eruptions in the Pribilof Islands began at St. George Island about 2.1 Ma and continued there for about 0.6 Ma (Cox et al., 1966). About 1 Ma after the initial eruption at St. George, volcanic eruptions began building St.

Paul Island, and have continued nearly to the present (Cox et al., 1966). Dredge samples from the Pribilof Ridge between St. George and St. Paul Islands have yielded basalts of an age intermediate between dates from St. George and St. Paul (Simpson et al., 1979), suggesting a northwest progression in volcanism.

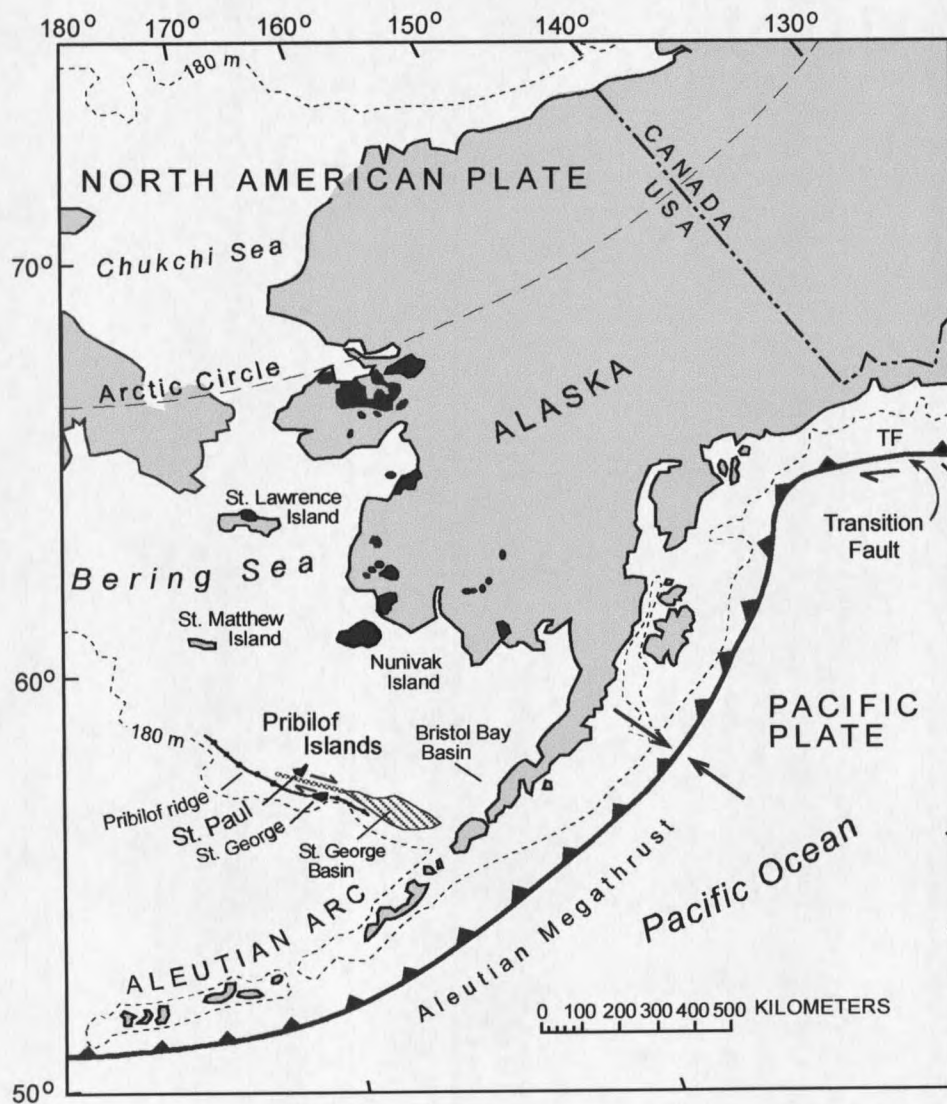


Figure 2. Tectonic setting of St. Paul Island. Black areas represent volcanic fields of the Bering Sea Basalt province. Adapted from Moll-Stalcup (1994a).

Pleistocene to Holocene in age, St. Paul is the youngest eruptive center in the Bering Sea basalt province, a group of approximately 15 late Cenozoic (<6 Ma) volcanic fields that are widely distributed behind the Aleutian arc front as eruptive centers along the Bering Sea coast of western Alaska and as islands on the Bering Sea shelf (Moll-Stalcup, 1994a, 1994b) (Fig. 2). Intraplate volcanism in the Bering Sea basalt province is associated with extension on the Bering Sea shelf and, in the Pribilof area, with extensional deformation and collapse of the Bering shelf margin (Marlow et al., 1976; Worrall, 1991; Cooper et al., 1992; Marlow et al., 1994; Plafker and Berg, 1994b; Moll-Stalcup, 1994a).

The Bering shelf margin was an active margin prior to early Tertiary time, when subduction of the Kula plate ceased (Marlow and Cooper, 1980; Plafker and Berg, 1994a; Marlow et al., 1994). Motion on the Beringian margin ceased about 50 Ma when subduction stepped to the south where the Pacific plate began to subduct beneath Alaska, trapping a fragment of the Kula plate behind the growing Aleutian arc (Hillhouse and Coe, 1994).

The North American and Pacific plates have since undergone dextral-oblique convergence along the northwest trending Transition fault and orthogonal convergence along the northeast trending Aleutian arc margin (Plafker and Berg, 1994a) (Fig. 2). Pacific plate motion is presently northwest relative to Alaska at rates from >4.9 cm/yr in southeastern Alaska to 7.7 cm/yr at the western end of the Aleutian arc (Plafker and Berg, 1994a). Some manifestations of the Pacific-North American plate interactions are (1) development of the Aleutian subduction zone and magmatic arc in early Tertiary time,

(2) basin formation associated with wrench faulting on the margin of the Bering Sea shelf, and (3) basaltic volcanism of the Bering Sea basalt province (Plafker and Berg, 1994a, 1994b) (Fig. 2).

Volcanism on the Bering Sea shelf margin appears to be controlled by mantle melting events related to continued extension and deep wrench faulting (Marlow and Cooper, 1980). The extension and wrench faulting have resulted in the formation of grabens such as St. George basin, which has developed along a margin-parallel dextral shear zone (Worrall, 1991; Cooper et al., 1992; Marlow et al., 1994; Plafker and Berg, 1994b) (Fig. 2). This shear zone strikes toward St. Paul Island, where the east-west orientation of tensional faults and eruptive centers suggests that this fault system, with a long history of past movement, is still active (Hopkins, 1976). Therefore, it appears that Quaternary volcanism on St. Paul Island is related to the ongoing interaction between the Pacific and North American plates (Cooper et al., 1992; Plafker and Berg, 1994a, 1994b; Plafker et al., 1994; Marlow et al., 1994).

Geology of St. Paul Island: Previous Work and Current State of Knowledge

St. Paul Island formed from both effusive and explosive eruptions of basaltic lavas. Early eruptions constructed a platform of nearly horizontal, stacked lava flows that rise to about 60 m above the sea. Barth (1956) suggested that these platform-building eruptions were mostly from subsequently buried fissures. Between the layered lava flows, in minor amounts, are intercalated layers of pyroclastic materials and sediments mixed with

reworked tephra, evidence that explosive eruptions were also a part of the early eruptive history of St. Paul Island (Barth, 1956).

The surface of St. Paul consists of more than fifteen scoria and spatter cones that rise 30 to 100 m above their bases and are surrounded by small shields of coalescing low viscosity lava flows (Fig. 3). St. Paul has a shoreline of headlands, sandy beaches, and wave-eroded cliffs. Seaward of the coastal cliffs are narrow beaches of angular to well-rounded basaltic boulders and, at some sites, the tessellated horizontal surfaces of eroded columnar basalt flows. Sandy beaches are located in areas where lava flows are too near sea level to form coastal cliffs. Three promontories, Reef Point, Tolstoi Point, and Zapadni Point, extend seaward from the southern shore of the island. These promontories, composed of layers of older platform lavas, are extensively faulted and tilted in contrast to the younger lava flows on the island's surface (Cox et al., 1966; Hopkins, 1976).

A central highland spans the island from east to west. Hopkins (1976) suggests that the eruptive centers aligned along this highland are rift related. The youthful volcanic topography of the central highland is marked by sharp, undissected cinder cones (Cox et al., 1966) where volcanic rocks have been little modified by mass wasting and erosion is minimal (Cox et al., 1966). Astride the highland, in the center of the island, Bogoslof Hill rises to a height of 180 m (590 feet). Bogoslof Hill was credited by Stanley-Brown (1892) with being the source of the most voluminous lava flows on the island. Surfaces of the lava flows on St. Paul have been fractured into boulders by frost-riving during intervals of more severe climate in the past, and the sharp outlines of the cinder cones

continue to be softened by geliturbation (Hopkins and Einarsson, 1966). There is no evidence that St. Paul has ever been glaciated (Hopkins and Einarsson, 1966).

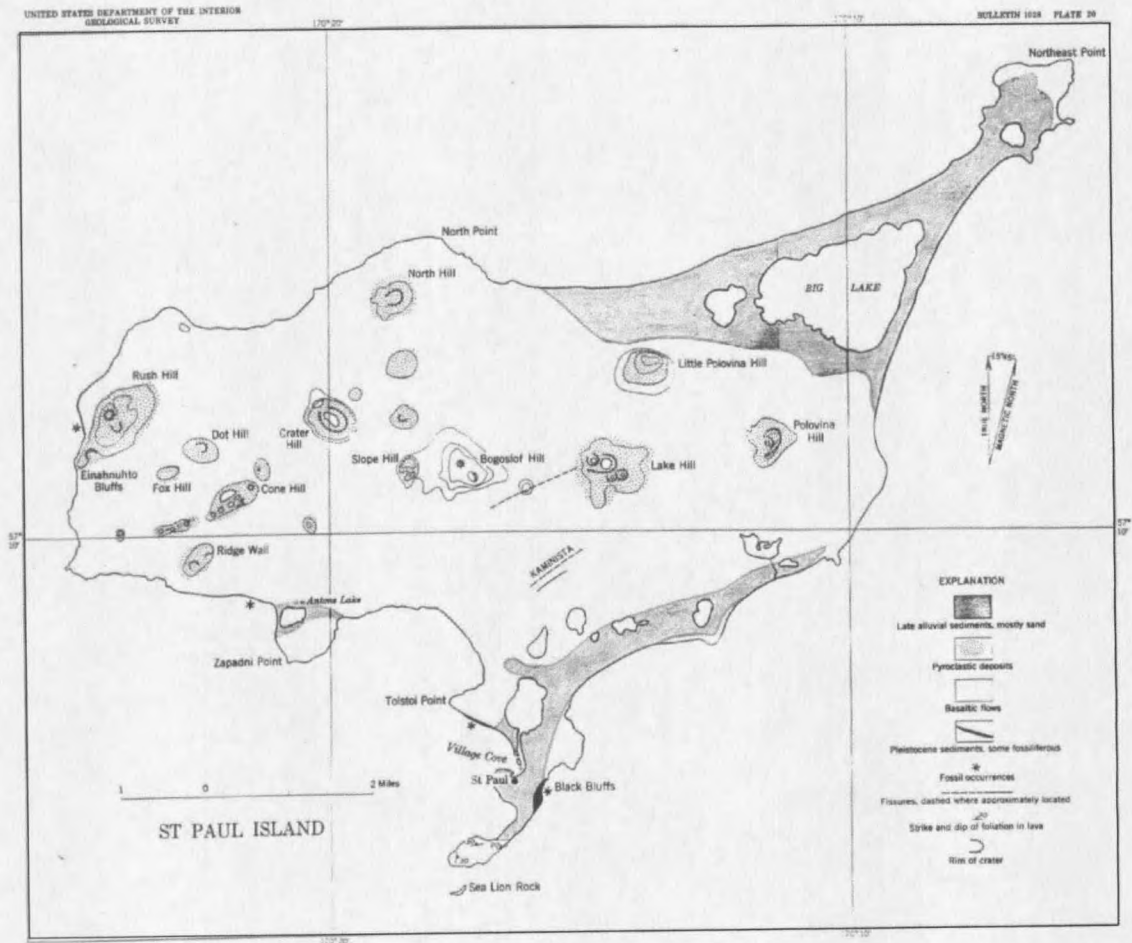


Figure 3. Barth's geologic map of St. Paul Island. From Barth (1956).

Evidence for a hydromagmatic eruption at Black Bluffs, a wave-eroded cone just east of the village of St. Paul, was noted by Stanley-Brown (1892) and Dawson (1894). These workers describe the stratification of the cone as well as the fossiliferous fragments of marly clay-rock, or calcareous argillite, torn from the sea floor during the eruption and

distributed throughout the layers of basaltic scoria and ash of the cone. Barth (1956) noted the polymict character and cross-bedding of deposits at Black Bluffs, and interpreted them as sediments transported by ice and deposited in water.

Sedimentary deposits on St. Paul Island range from layers of marine, eolian, and colluvial sediments intercalated in the layers of platform lavas, to extensive covers of eolian silt on most of the lava flows, to coastal sand dunes occurring on the eastern portion of the island (Barth, 1956; Cox et al., 1966; Hopkins, 1967a; Hopkins, 1976). The dunes, now mostly stabilized by vegetation, do not appear to have been faulted (Hopkins, 1976). Hopkins attributes the source of the eolian sediments to the Bering land bridge that was exposed during times of lowered sea level. During the platform building stage, marine transgressions related to glacial intervals deposited fossiliferous marine and beach gravel sediments on St. Paul Island (Cox et al., 1966; Hopkins, 1967a). The oldest of the marine sediments are from the Anvilian transgression (probably <1.9 to >0.7 Ma) (Hopkins, 1967). Fossiliferous marine sediments, probably of Anvilian age, are exposed on St. Paul Island at Tolstoi Point and are possibly incorporated into the base of the tuff cone at Black Bluffs (Hopkins, 1967a). A third possible location of this sedimentary deposit is beneath the village hill. In 1818, a well drilling operation, located near the north end of St. Paul village, bored into a layer of "gray marl" at 3 m above sea level (Hanna, 1919). However, a relationship between the calcareous, fossil-bearing clay blocks in Black Bluffs (described by Stanley-Brown, 1892), the marl under the village hill (Hanna, 1919), and the Anvilian sediments at Tolstoi Point (Hopkins, 1967a) has not been established.

The type locality for the middle Pleistocene Einahnuhtan transgression [<300 ka and >100 ka (Hopkins, 1976a)] is on western St. Paul Island at Einahnuhto Bluffs where marine sediments are emplaced over the stratigraphically lowest lava flow exposed beneath the bluffs (Hopkins, 1967a) [this lava flow was dated at 0.360 ± 0.10 Ma by Cox et al. (1966)]. At Einahnuhto Bluffs, fossiliferous beach and littoral Einahnuhtan sediments are interbedded with pillow lavas (Hopkins, 1967a; Lee-Wong et al., 1979) and unconformably overlain by younger boulder beach gravel of Kotzebuan age (~ 175 Ka) (Hopkins, 1967a). Hopkins (1967a) describes a wave-cut scarp as high as +33 m on Tolstoi Point as being carved during the Kotzebuan transgression. Fossiliferous marine sediments from the Einahnuhtan transgression are also exposed in sea cliffs at Tolstoi Point and Zapadni Point (Hopkins, 1967a). Fauna in Einahnuhtan sediments are, with few exceptions, modern (Hopkins, 1967a). Dawson (1894) described a chain of dunes southeast of Big Lake that appear to follow the subtle break-in-slope, which he attributed to changing sea level. Sea level has remained near its present level since about 3,000 BC (Hopkins, 1967a). The interested reader is directed to Hopkins (1976a) for an in-depth discussion of the various changes in sea level that affected St. Paul Island. Marine sediments and fossils of St. Paul Island are also described in some detail in earlier works (Stanley-Brown, 1892; Dall, 1899; Hanna, 1919; Washington and Keyes, 1930; Hopkins, 1967a; Hopkins, 1976).

St. Paul Island has no surface streams, as the highly permeable volcanic rocks allow the infiltration of most precipitation (Hopkins and Einarsson, 1966). However, fresh water is found in lakes, located most often in or near the sand dunes. A few small lakes

have formed in the craters of volcanic cones such as Crater Hill and Lake Hill. The largest body of fresh water, Big Lake, formed inside the tombolo that connects Northeast Point to the main body of St. Paul Island. Formation of this tombolo was completed in historic time, as early settlers on St. Paul, in the late 1700's, required boats to travel from the main island to Northeast Point (Elliott, 1881; Father Michael Lestenkof, 2000, personal commun.). Northeast Point was formerly called "Novastoshnah", from the Russian meaning, "of recent growth" (Elliott, 1881). Antone Lake, on the northwest part of Zapadni Point, was likely formed by the sea ice crowding boulders into a rampart, as described by Stanley-Brown (1892), and forming the dam that contains the lake.

In previous work on St. Paul, Barth (1966), who published the first geologic map of the island (Fig. 3), recognized multiple volcanic vents, but did not map any separate lava flows. Barth's (1956) map merely distinguishes lavas from sand dunes and shows the locations of some vents with pyroclastic deposits on St. Paul. A preliminary report by Lee-Wong et al. (1979) includes an unpublished reconnaissance sketch map of St. Paul by Hopkins and Einarsson, dated 1965. This map shows faults and breaks out volcanic rocks into four units: (1) Rush Hill, (2) Bogoslof Hill, and lavas both (3) older and (4) younger than Bogoslof Hill, the latter including the Fox Hill lava flow. Cox et al. (1966) mapped some faults and eruptive centers, including Fox Hill and the Fox Hill lava flow, while studying geomagnetic polarity epochs on St. Paul lavas and collecting samples for K-Ar radiometric age determinations. In an investigation of geologic hazards related to locating an oil pipeline and oil trans-shipment facility on St. Paul, Hopkins (1976) studied the history and frequency of faulting and volcanic eruptions on the island.

Hopkins' (1976) study of the fault history of St. Paul Island cited no clear evidence that faulting has affected stabilized sand dunes. Hopkins (1976) estimates the ages of the dunes to be around 10,000 to 12,000 years old and the rate of displacement on individual faults to be approximately one meter per 10,000 years. [Despite considerable effort, Hopkins' (1976) fault map from this study could not be obtained.] Hopkins (1976) concluded that faulting is an ongoing process and estimated a 10,000 year eruptive interval for volcanic activity on St. Paul Island.

Petrographic and compositional studies have been done on St. Paul rocks by several workers (Washington and Keyes, 1930; Barth, 1956; Cox et al., 1966; Kay et al., 1978; Lee-Wong et al., 1979). Magmas erupted at St. Paul have been classified by Barth (1956) as alkalic basalts and basanites, both containing phenocrysts of olivine and augite \pm plagioclase, with occasional inclusions of olivine nodules. Cox et al. (1966) reported not only frequent ultramafic inclusions, but also granitic xenoliths, with both types sometimes occurring together. In a singular finding, Barth (1956) located a small amount of rhyolitic pumice ($\text{SiO}_2 = 69.09$ wt%: Barth's (1956) analysis) high on the east slope of Polovina Hill. Pribilof basalts were early recognized as having chemistry comparable to that of ocean island basalts in the Pacific Ocean by Washington and Keyes (1930). This was corroborated by Kay et al. (1978), who found that Pribilof basalts were isotopically similar to seamount lavas erupted in an intraplate environment; they attributed the Pribilof magma source region to the underlying asthenospheric mantle. Lee-Wong et al. (1979) conducted petrographic and geochemical studies using previously collected samples of St. Paul rocks. They interpreted the wide range of MgO values (4.85 to

14.64 wt%) for the silica-poor (44.23 to 46.79 wt%) rocks as reflecting substantial differentiation. Lee-Wong et al. (1979) noted a trend of decreasing MgO content with decreasing age of St. Paul magmas; they also commented on the consistently low MgO content of the Bogoslof Hill lavas. More recently, Moll-Stalcup (1994a, 1994b) described St. Paul Island as a part of the Bering Sea basalt province, the product of intraplate volcanism related to regional north-south extension in the Bering Sea region (Moll-Stalcup, 1994a). Moll-Stalcup (1994a) suggested that the rock underwent little, if any, differentiation. Most recently, Winer and Feeley (1997) and Feeley and Winer (1999) described petrographic and geochemical evidence for fractionation of Quaternary basalts on St. Paul, and argued for the development of shallow crustal magma chambers beneath the island.

Ages of rocks erupted on St. Paul Island are all within the Bruhnes chron of normal polarity (<780 ka) (Cox et al., 1966). Absolute and relative age determinations by Cox et al. (1966) put the ages of lavas on St. Paul Island from 0.360 ± 0.10 Ma to nearly the present [radiometric age determinations from Cox et al. (1966) are discussed below in Chapter 3]. A sediment core from the lake in the Lake Hill crater yielded a radiocarbon age determination of >17,800 years BP (Colinvaux, 1981). This age is poorly constrained because of the introduction of groundwater into the sediment (Colinvaux, 1981). Washington and Keyes (1930) cited a report by Landgrebe (1855) of "flames rising from the sea" northeast of the Pribilof Islands, and also of a submarine eruption recorded as occurring in the vicinity of St. George Island (Sapper, 1917). Barth (1956) also cited Landgrebe (1855), but regarded any assertions of such recent volcanic activity

in the area as inconclusive. The fact that lava has flowed from a crater on Bogoslof Hill was noted by Stanley-Brown (1892) and Barth (1956). However, no historic eruptions have occurred at St. Paul Island.

METHODS

Mapping and Sample Collection

Fieldwork on St. Paul Island was done during three weeks in June 1998, and one week in September 2000. Field relations were mapped using NOAA map # 16382 (1:50,000) as a base map and aerial color photographs (1:24,000), acquired June, 1993, by Aeromap, Anchorage, Alaska. The base map was enlarged for use in the field. The aerial photographs were studied at Montana State University prior to fieldwork, and were utilized in the field. Where possible, individual lava flows and their source vents were mapped. Mappable eruptive units include an assemblage of volcanic products inferred to have erupted from a single common vent, from several closely spaced vents, or from several more widely spaced vents related by structural continuity. For volcanic centers with a series of eruptive events from a common center, to the extent possible, separate flows are delineated on the geological map (Plate 1). Access to some coastal locations was limited by not only the steepness of the near vertical cliffs, but also by the presence of large, territorial, and belligerent northern fur seal bulls on their breeding grounds. The geologic map made in the field has been converted into digital form.

In total, seventy-eight samples were collected. Of these samples, 72 are volcanic rock samples of 1 to 2 kg each; four are beach sand; one is about 4 kg of organic carbon-containing sediment; and one is fossil shells. Rock samples were collected from the densest and freshest rocks available and trimmed of weathered surfaces as necessary.

X-ray Fluorescence

Approximately 100 grams of each of 37 selected rock samples were sent to the WSU GeoAnalytical Laboratory at Washington State University, Pullman, Washington. These samples were analyzed by X-ray fluorescence (XRF) for major element oxides and trace elements (Table 1) with all Fe expressed as FeO. XRF was done using techniques outlined by Johnson et al. (1999).

Petrography

Seventy-two billets were sent to Wagner Petrographic, Provo, Utah, for preparation as petrographic thin sections. Thin sections were examined using a polarizing petrographic microscope. Microscopic data consists of two types: qualitative textural data (described below) and quantitative modal data (Table 1). Modal phenocryst percentages were determined by point counting 1100 to 1200 points per thin section. Phenocrysts are defined as crystals ≥ 0.3 mm in the longest dimension. Because these basaltic rocks are all vesicular to some extent, vesicles were included in the modal analysis and then their proportion was subtracted from the total numbers of counts to give the dense rock equivalent.

Geochronology

One sample (SP98-64) of organic carbon-containing sediment, exposed beneath a lava flow, was collected with a shovel and stored in a sealed plastic bag. Sediment was collected from the upper one third of the deposit, but not from the top few centimeters, where complete combustion of organic matter occurs (Kuntz et al., 1986b). Beta Analytic Inc., Radiocarbon Dating Services, Miami, Florida, analyzed the carbon sample. They found that the amount of carbon in the sample was very small, requiring them to convert the sample carbon to graphite and then to count the radiocarbon atomically using an accelerator mass spectrometer (AMS). This method provided sufficient carbon for reliable measurements and all analytical steps went normally. Details of the analytical procedures are explained in Appendix A.

GEOLOGY OF ST. PAUL ISLAND

This chapter on the geology of St. Paul Island includes geochronology, chemical classification of the rocks, major and trace element compositions, modal and normative minerals, rock names, and the new geological map. Map units are described and interpreted.

Ages of Rocks on St. Paul Island

Ages of rocks on St. Paul Island are bracketed by two events, a geomagnetic polarity transition and the eruption of the youngest lava flow on the island. Geomagnetic polarity studies conducted by Cox et al. (1966) determined that all volcanic rocks forming St. Paul Island erupted during the Bruhnes chron of normal polarity, 780 Ka to the present. Using K-Ar determinations on the island platform lavas, Cox et al. (1966) also obtained intermediate dates ranging from 0.36 ± 0.10 Ma to 0.096 ± 0.10 Ma. A new radiometric age-date from this study verifies that St. Paul Island has erupted in the very recent geologic past. A high-precision AMS radiocarbon age-date obtained on organic carbon-bearing sediments located beneath the Fox Hill lava flow, shows that the youngest eruption on St. Paul Island occurred $3,230 \pm 40$ years before the present at Fox Hill.

Classification and Composition of St. Paul Rocks

Most volcanic rocks erupted on St. Paul Island range from basanites and tephrites to trachybasalts and basalts (Fig. 4). In addition, one rare trachyte magma erupted from Polovina Hill. All volcanic rocks are alkaline according to the nomenclature of MacDonald and Katsura (1964). Samples were collected from eighteen eruptive centers as well as from lava flows for which source vents were not identified. Due to emplacement mechanisms and in-flow mixing of very low viscosity pahoehoe lava flows (Hon et al., 1994; Peterson et al., 1994; Calvari and Pinkerton, 1999; Kilburn, 2000), each sample is considered to be representative of the lava flow as a whole. As a test of this premise, four samples from the Fox Hill lava flow (SWPT1, SWPT2, SWPT3, and FXH1) were analyzed. Within analytical error, all are identical in chemical composition. Most samples, except for those collected along the sea cliffs and those from eruptive centers where only tephra was exposed, were taken from flow surfaces; cross-sections of inland lava flows do not exist, due to little erosion.

Major and trace element analyses of St. Paul rocks are presented in Table 1. Because of the limited range of SiO₂ (43.11 to 47.30 wt%) and larger range of MgO contents (14.39 to 4.25 wt%), the basaltic rocks are ordered by decreasing MgO content. Modal mineralogy is included in Table 1. Also included in the table are analyses of the rare trachyte magma (SP98-35), erupted from Polovina Hill, and two xenoliths (SP98-51X and SP98-43X). Modal minerals are presented in Table 1 and normative minerals and rock names are presented in Table 2.

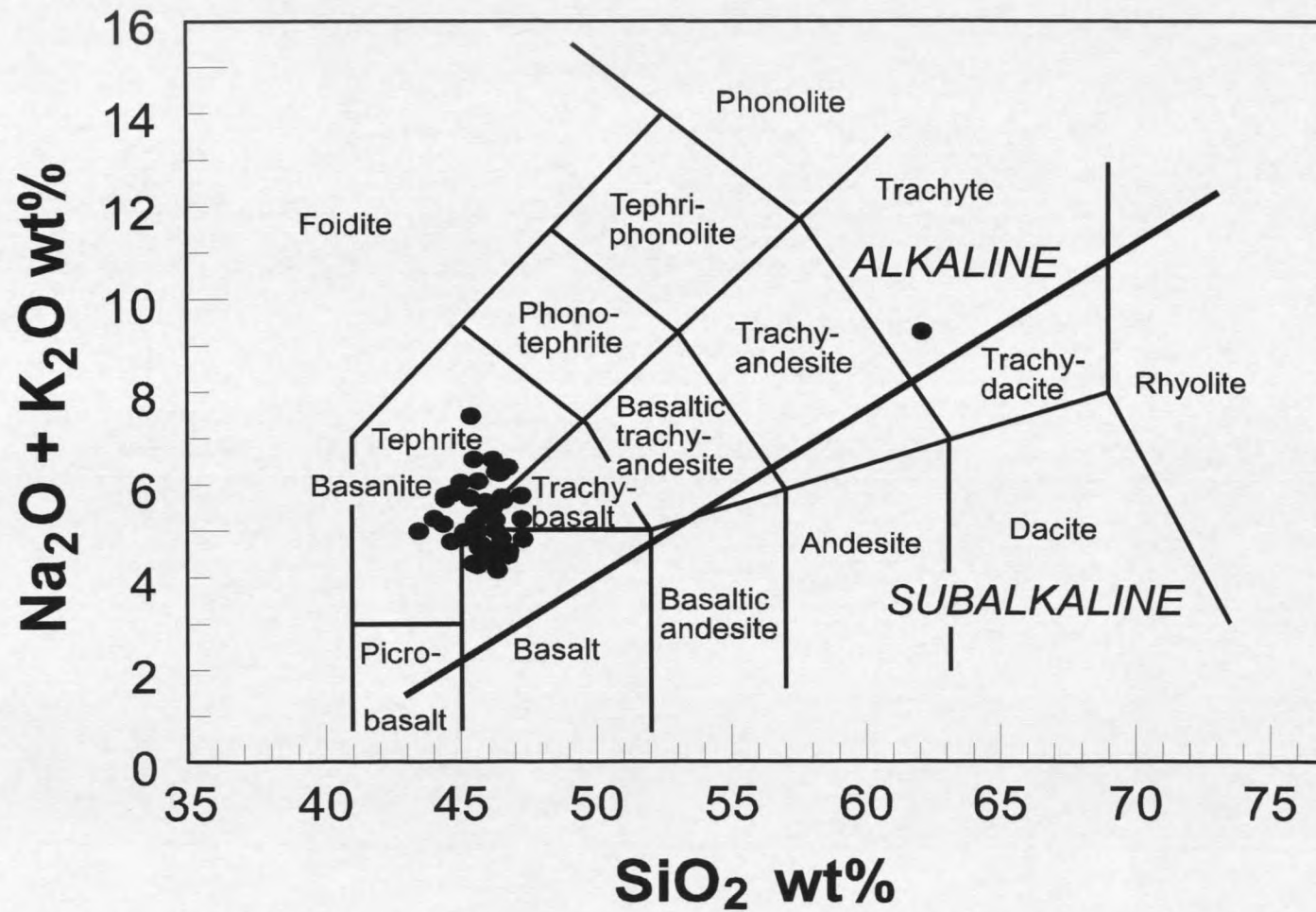


Figure 4. Classification of the rocks. Chemical classification scheme and nomenclature of St. Paul volcanic rocks using the total alkalis versus silica (TAS) diagram of le Maitre et al. (1989). The straight heavy line separates alkalic from subalkalic rocks (MacDonald and Katsura (1964)).

Table 1. Major element, trace element, and modal analyses of volcanic rocks and xenoliths from St. Paul Island, Alaska

Map unit Sample #	UPL 9825	UPL 9870	UPL 9816	NoH 9837	RW 9843	POL POL 1	UPL SWPB 1	UPL 9822
Major element oxides (wt%)								
MgO	14.39	13.95	12.45	12.36	12.09	12.02	11.95	11.88
SiO ₂	45.08	45.61	45.67	44.01	45.11	43.11	44.35	45.82
Al ₂ O ₃	12.41	12.52	13.20	12.95	12.96	13.29	13.22	13.39
TiO ₂	2.241	2.134	2.325	2.825	2.534	3.006	2.376	2.377
[†] FeO	11.01	10.88	11.40	12.30	11.83	12.30	12.16	11.50
MnO	0.172	0.175	0.169	0.174	0.173	0.172	0.168	0.169
CaO	9.38	9.59	9.58	9.38	9.65	9.78	9.86	9.97
K ₂ O	1.31	1.16	1.28	1.60	1.33	1.39	1.45	1.21
Na ₂ O	3.47	3.03	3.31	3.60	3.51	3.59	3.63	3.25
P ₂ O ₅	0.497	0.430	0.394	0.592	0.450	0.566	0.523	0.438
Total	99.96	99.48	99.78	99.79	99.63	99.22	99.69	100.01
Trace elements (ppm)								
Ni	356	345	276	268	272	241	270	239
Cr	535	460	479	377	356	332	521	438
Sc	23	21	23	27	22	28	31	21
V	251	243	241	266	240	295	263	253
Ba	174	116	118	159	187	291	272	132
Rb	13	12	13	17	17	17	16	13
Sr	618	500	488	680	509	663	675	522
Zr	170	154	159	190	156	190	181	146
Y	18	18	19	19	21	19	19	19
Nb	40.5	35.0	39.1	47.8	45.3	48.5	44.2	38.1
Ga	16	17	20	20	23	20	16	20
Cu	44	47	50	47	57	45	49	30
Zn	81	88	89	93	98	91	82	87
Pb	1	3	3	3	1	0	2	2
La	16	11	19	14	14	41	30	20
Ce	41	29	39	48	55	49	50	41
Th	5	2	5	2	6	7	7	2
³ Modal percent phenocrysts								
plag	0.4	0.1	0.1	0	0	0.4	1.1	3.1
olivine	21.3	22.9	17.3	17.9	17.1	15.0	17.9	19.6
cpx	3.2	5	0.8	2.7	0.1	7.3	0.9	0.3
oxide	0.4	0	0	0	0	0.3	0.5	0
total	25.3	28	18.2	20.6	17.2	23.0	20.4	23

[†] Total Fe expressed as FeO

³ Crystals with greatest dimension greater than or equal to 0.3mm counted as phenocrysts

† Denotes values >120% of highest standards

Table 1. Continued

	RW 9842	UPL 9814	UPL 9810	LH 9833	UPL ERP 2	RiH 9877	CH 9851
MgO	11.76	11.68	11.60	11.20	11.06	11.04	10.91
SiO ₂	45.62	46.24	46.18	45.53	45.93	45.73	45.14
Al ₂ O ₃	13.21	13.24	13.39	13.20	13.42	13.81	13.74
TiO ₂	2.572	2.360	2.367	2.687	2.522	2.549	2.650
¹ FeO	11.24	11.81	11.79	11.76	12.54	10.24	11.74
MnO	0.175	0.171	0.173	0.176	0.173	0.172	0.186
CaO	9.81	9.70	9.58	9.80	9.51	10.27	9.81
K ₂ O	1.34	1.21	1.15	1.36	1.30	1.61	1.16
Na ₂ O	3.59	3.05	3.35	3.43	3.15	3.63	3.75
P ₂ O ₅	0.460	0.451	0.448	0.545	0.494	0.567	0.466
Total	99.78	99.92	100.02	99.69	100.1	99.62	99.55
Ni	266	239	238	241	228	229	226
Cr	360	325	322	323	289	368	281
Sc	29	25	22	27	25	28	27
V	241	227	229	241	239	279	244
Ba	194	157	147	195	270	160	164
Rb	18	12	13	16	13	12	14
Sr	515	551	540	569	542	731	554
Zr	160	153	152	173	160	184	171
Y	22	20	20	22	21	21	21
Nb	45.4	39.5	38.9	47.8	43.2	40.4	40.8
Ga	20	22	20	21	23	19	17
Cu	60	45	49	50	56	42	51
Zn	94	99	95	103	104	87	100
Pb	0	0	2	4	0	3	0
La	19	16	17	19	21	18	23
Ce	47	46	56	50	52	58	49
Th	5	6	5	5	5	6	6
plag	0	30.3	21.3	0.4	9.1	3.7	0.9
olivine	18.5	17.1	14.8	11.7	15.1	17.4	9.7
cpx	0	6.9	3.2	0.4	1.2	4.1	1.7
oxide	0	2.1	0	0	0	0	0
total	18.5	56.4	39.3	12.5	25.4	25.2	12.3

Table 1. Continued

	KAM KAM 1	UPL ERP 1	UPL 9813	H404 9853	H255 9840	Hill 255 9841	PyC 9845
MgO	10.87	10.68	10.55	10.52	10.32	10.09	9.99
SiO ₂	45.46	45.77	46.50	44.65	46.78	46.76	46.35
Al ₂ O ₃	13.51	13.54	13.87	14.03	13.59	13.63	13.47
TiO ₂	2.455	2.525	2.481	2.846	2.373	2.427	2.304
¹ FeO	13.48	13.47	11.50	10.80	12.04	12.02	12.58
MnO	0.171	0.176	0.172	0.180	0.176	0.177	0.168
CaO	9.62	9.45	9.58	10.68	9.55	9.65	9.38
K ₂ O	1.22	1.21	1.19	1.57	1.06	1.01	0.88
Na ₂ O	3.01	3.41	3.58	3.13	3.44	3.39	3.21
P ₂ O ₅	0.469	0.484	0.456	0.548	0.454	0.444	0.365
Total	100.26	100.72	99.88	98.95	99.78	99.60	98.70
Ni	216	211	202	191	211	205	197
Cr	308	292	314	326	266	265	250
Sc	21	26	24	31	21	28	20
V	229	231	237	295	220	240	207
Ba	244	249	146	179	130	128	98
Rb	14	13	13	14	11	10	8
Sr	581	547	528	669	511	474	414
Zr	165	163	155	189	150	148	135
Y	20	21	20	21	21	21	20
Nb	38.9	41.5	37.5	47.2	36.6	35.9	28.8
Ga	20	20	19	20	19	21	20
Cu	48	52	48	44	57	66	45
Zn	101	98	96	89	101	104	99
Pb	1	1	2	0	0	4	3
La	16	13	25	30	17	12	23
Ce	48	58	37	67	37	50	35
Th	5	3	3	5	3	3	5
plag	39.7	13.6	41.3	0	0.8	0	9.8
olivine	19.0	13.9	17.6	10.2	12.6	9.7	11.9
cpx	24.4	2.1	14.4	3.5	0.1	0	8.3
oxide	5.9	0	3.5	0	0	0	0
total	89.0	29.6	76.8	13.7	13.5	9.7	30

Table 1. Continued

	PyC 9854	UPL 9871	Upl 9819	PyC 9852	ALF 9831	ALF 9875	CHVC 9846
MgO	9.66	9.43	8.89	8.74	8.23	8.05	7.56
SiO ₂	45.34	46.27	47.25	45.00	45.53	45.91	46.28
Al ₂ O ₃	14.69	14.23	14.79	14.77	15.16	15.28	15.24
TiO ₂	2.781	2.558	2.474	3.037	2.879	2.941	2.886
¹ FeO	10.67	11.23	10.90	11.26	12.02	11.55	11.25
MnO	0.175	0.173	0.169	0.174	0.173	0.174	0.172
CaO	9.54	9.91	9.55	10.22	9.56	9.74	10.56
K ₂ O	1.75	1.20	1.49	1.72	1.52	1.63	1.50
Na ₂ O	3.90	3.75	3.70	4.26	3.62	3.93	3.67
P ₂ O ₅	0.575	0.492	0.401	0.651	0.549	0.560	0.540
Total	99.08	99.25	99.62	99.83	99.24	99.76	99.66
Ni	189	155	151	136	73	67	84
Cr	272	304	297	233	215	227	199
Sc	23	29	26	26	27	23	30
V	257	257	247	286	266	266	281
Ba	215	135	125	211	163	156	160
Rb	20	11	17	19	13	15	14
Sr	672	571	515	744	697	714	635
Zr	206	165	197	204	205	198	192
Y	23	22	21	22	21	21	22
Nb	53.1	37.3	45.1	49.5	45.5	42.8	43.0
Ga	22	20	21	21	24	23	22
Cu	47	37	46	39	32	30	57
Zn	90	103	92	89	99	97	91
Pb	1	1	2	1	2	3	2
La	25	24	20	29	27	19	8
Ce	66	42	58	66	57	48	49
Th	4	4	6	5	2	4	3
plag	0	53.8	19	1.3	22	25.7	14
olivine	11.4	16.3	11	10.1	11.1	8	7.2
cpx	5.1	17.5	0.4	5	2.2	5.3	6.3
oxide	0	2	0	0	0	1.2	0
total	16.5	89.6	30.4	16.4	35.3	40.2	27.5

Table 1. Continued

	HH 9804	CHVC 9856	FXH SWPT 2	FXH FXH 1	RuH 9878	FXH SWPT 3	FXH SWPT 1
MgO	7.54	7.42	7.40	7.40	7.36	7.27	7.20
SiO ₂	47.30	46.19	44.73	44.43	45.80	44.43	44.52
Al ₂ O ₃	15.40	15.35	15.02	15.09	15.93	15.06	15.06
TiO ₂	2.534	2.865	3.394	3.402	3.045	3.405	3.394
¹ FeO	11.27	11.20	13.07	12.83	11.12	12.64	13.07
MnO	0.174	0.175	0.168	0.169	0.180	0.169	0.169
CaO	10.22	10.33	9.71	9.65	9.12	9.67	9.63
K ₂ O	1.13	1.54	1.77	1.80	2.39	1.72	1.78
Na ₂ O	3.62	3.90	3.98	3.89	3.61	3.90	3.93
P ₂ O ₅	0.463	0.556	0.550	0.558	0.779	0.564	0.561
Total	99.65	99.53	99.79	99.22	99.34	98.83	99.31
Ni	86	83	68	71	96	70	69
Cr	234	162	122	119	139	118	115
Sc	25	27	24	23	24	27	30
V	239	283	294	299	260	274	292
Ba	123	140	269	280	294	314	291
Rb	14	14	15	16	24	14	15
Sr	535	642	673	677	†931	676	677
Zr	174	195	196	198	246	198	200
Y	24	23	21	21	23	22	21
Nb	39.3	43.5	43.2	45.3	64.5	44.3	43.7
Ga	23	24	24	26	23	22	23
Cu	41	56	28	43	24	42	37
Zn	100	93	93	98	91	94	96
Pb	0	0	0	1	4	0	2
La	27	20	17	21	28	16	29
Ce	51	64	54	49	78	42	63
Th	6	5	5	3	5	2	4
plag	22.4	13.5	3.5	3.6	0.8	1.1	7.1
olivine	6.6	9.7	10.4	11.3	5.7	8.3	8.1
cpx	3.4	4.2	0.4	2.0	0.4	0.3	1.5
oxide	0	0	0.4	0.2	0	0	0.6
total	32.4	27.4	14.7	17.1	6.9	9.7	17.3

Table 1. Continued

	RuH 9818	CHVC 9858	CHVC 9849	RuH 9823	CHVC 9857	BHVC 9847	BHVC 9873
MgO	6.91	6.80	6.72	6.46	6.40	6.01	5.69
SiO ₂	45.49	46.38	46.52	45.37	46.50	46.89	46.45
Al ₂ O ₃	16.00	15.77	15.71	16.23	15.85	15.97	16.37
TiO ₂	3.046	2.955	2.941	3.241	2.995	3.042	3.208
[†] FeO	11.15	10.67	11.11	11.10	10.99	10.64	10.99
MnO	0.174	0.176	0.173	0.181	0.174	0.170	0.173
CaO	9.68	10.23	10.06	8.79	10.18	10.62	9.91
K ₂ O	2.29	1.58	1.58	2.52	1.64	1.63	1.85
Na ₂ O	4.19	3.99	4.08	4.94	4.02	4.07	4.33
P ₂ O ₅	0.713	0.571	0.579	0.861	0.591	0.574	0.645
Total	99.65	99.12	99.47	99.70	99.34	99.61	99.61
Ni	52	70	72	58	65	32	23
Cr	103	114	105	78	101	119	79
Sc	24	23	22	17	19	24	26
V	275	283	272	262	280	290	288
Ba	205	157	157	287	153	148	186
Rb	17	13	13	24	14	15	18
Sr	†895	648	651	†950	661	718	†799
Zr	233	200	198	262	203	210	214
Y	23	24	22	24	23	22	21
Nb	56.7	45.3	44.9	67.5	46.3	46.2	47.3
Ga	24	23	21	26	20	23	21
Cu	25	57	65	18	63	47	30
Zn	88	92	94	91	94	95	92
Pb	4	2	2	5	0	1	4
La	29	16	22	32	29	21	28
Ce	72	59	71	80	61	66	62
Th	4	3	5	2	6	4	2
plag	0.4	12.4	7.3	2.2	13.9	30	27.3
olivine	5.2	5.9	5	5.2	5.4	2.7	4.8
cpx	1.7	2.2	0.1	0	0.3	13.8	2.5
oxide	0	0	0	0	0	0	0
total	7.3	20.5	12.4	7.4	19.6	46.5	34.6

Table 1. Continued

	BHVC 9826	BHVC 9872	BHVC 9827	POL 9835	Crater Hill 9851X	Ridge W. 9843X
MgO	5.37	5.29	4.25	1.15	4.70	0.26
SiO ₂	46.31	46.75	46.18	62.06	50.28	74.05
Al ₂ O ₃	16.35	16.49	15.51	16.72	19.32	15.46
TiO ₂	3.244	3.310	3.877	0.890	1.671	0.058
¹ FeO	11.70	10.65	12.43	4.42	8.24	0.57
MnO	0.170	0.174	0.187	0.081	0.145	0.005
CaO	9.94	10.05	9.69	4.10	9.12	4.92
K ₂ O	1.87	1.87	2.22	4.34	0.39	0.52
Na ₂ O	4.33	4.44	4.26	4.89	4.64	4.05
P ₂ O ₅	0.660	0.649	0.784	0.208	0.192	0.037
Total	99.95	99.68	99.39	98.86	98.70	99.93
Ni	19	18	4	4	14	10
Cr	62	65	36	0	34	0
Sc	28	24	20	12	25	9
V	280	287	324	60	234	15
Ba	193	182	194	690	35	82
Rb	14	14	21	47	3	10
Sr	†819	735	685	451	747	465
Zr	223	221	260	147	78	43
Y	24	23	28	24	11	2
Nb	50.0	50.6	61.2	8.8	8.1	4.5
Ga	25	23	27	19	21	14
Cu	32	32	39	32	72	26
Zn	97	99	112	43	76	2
Pb	0	2	3	6	0	3
La	15	28	42	15	7	0
Ce	77	62	86	28	22	31
Th	9	2	7	0	0	0
plag	30.1	19	8.9	17.4		
olivine	2.9	4.1	2.1	0.1		
cpx	5.1	0.9	0.6	0.1		
oxide	0.4	0	0	2.1		
total	38.5	24	11.6	19.7		

Table 2. CIPW Calculated Normative Minerals in Weight Percent and Rock Names

Map Unit	UPL	UPL	UPL	NoH	RW	POL	UPL	UPL	RW	UPL
SAMPLE	9825	9870	9816	9837	9843	POL 1	SWPB 1	9822	9842	9814
Normative										
Q	0.00	0.00	0.00	0.00	0.00	0.00	0.00	0.00	0.00	0.00
or	7.72	6.87	7.55	9.43	7.86	8.24	8.56	7.12	7.90	7.13
ab	11.55	14.81	14.88	10.01	13.45	8.93	9.53	15.55	14.68	18.22
an	14.37	17.16	17.35	14.42	15.67	16.10	15.48	18.30	15.94	18.81
lc	0.00	0.00	0.00	0.00	0.00	0.00	0.00	0.00	0.00	0.00
ne	9.60	5.89	7.09	11.04	8.80	11.68	11.47	6.41	8.47	4.07
kal	0.00	0.00	0.00	0.00	0.00	0.00	0.00	0.00	0.00	0.00
C	0.00	0.00	0.00	0.00	0.00	0.00	0.00	0.00	0.00	0.00
di	22.85	22.00	21.94	22.42	23.31	22.96	23.98	22.42	23.56	20.97
hy	0.00	0.00	0.00	0.00	0.00	0.00	0.00	0.00	0.00	0.00
wo	0.00	0.00	0.00	0.00	0.00	0.00	0.00	0.00	0.00	0.00
ol	23.13	22.94	20.34	19.70	19.22	18.51	19.65	19.08	17.61	19.72
ac	0.00	0.00	0.00	0.00	0.00	0.00	0.00	0.00	0.00	0.00
mt	5.41	5.28	5.54	6.26	5.85	6.55	5.62	5.60	5.89	5.58
il	4.24	4.06	4.41	5.35	4.81	5.73	4.51	4.50	4.88	4.47
hem	0.00	0.00	0.00	0.00	0.00	0.00	0.00	0.00	0.00	0.00
ti	0.00	0.00	0.00	0.00	0.00	0.00	0.00	0.00	0.00	0.00
ap	1.15	1.00	0.91	1.37	1.04	1.32	1.21	1.01	1.06	1.04
Rock type*	basalt	basalt	basalt	basanite	basalt	basanite	basanite	basalt	basalt	basalt

*According to Le Maitre (1989)

Table 2. Continued

	UPL	LH	UPL	RiH	CH	KAM	UPL	UPL	H404	H255
SAMPLE	9810	9833	ERP 2	9877	9851	KAM 1	ERP 1	9813	9853	9840
Q	0.00	0.00	0.00	0.00	0.00	0.00	0.00	0.00	0.00	0.00
or	6.77	8.03	7.64	9.51	6.86	7.16	7.07	7.01	9.34	6.25
ab	18.05	15.96	17.92	13.29	15.30	16.69	17.20	19.67	12.17	21.67
an	18.03	16.59	18.55	16.63	17.24	19.62	17.87	18.21	19.72	18.48
lc	0.00	0.00	0.00	0.00	0.00	0.00	0.00	0.00	0.00	0.00
ne	5.52	7.06	4.66	9.44	8.91	4.67	6.14	5.71	7.84	4.01
kal	0.00	0.00	0.00	0.00	0.00	0.00	0.00	0.00	0.00	0.00
C	0.00	0.00	0.00	0.00	0.00	0.00	0.00	0.00	0.00	0.00
di	21.09	22.65	20.19	24.24	22.65	19.94	20.43	20.93	23.75	20.74
hy	0.00	0.00	0.00	0.00	0.00	0.00	0.00	0.00	0.00	0.00
wo	0.00	0.00	0.00	0.00	0.00	0.00	0.00	0.00	0.00	0.00
ol	19.46	17.30	19.34	14.88	16.92	20.52	19.67	16.96	14.13	17.71
ac	0.00	0.00	0.00	0.00	0.00	0.00	0.00	0.00	0.00	0.00
mt	5.58	6.06	5.80	5.87	6.02	5.70	5.77	5.76	6.34	5.61
il	4.48	5.10	4.77	4.84	5.03	4.63	4.74	4.70	5.44	4.50
hem	0.00	0.00	0.00	0.00	0.00	0.00	0.00	0.00	0.00	0.00
ti	0.00	0.00	0.00	0.00	0.00	0.00	0.00	0.00	0.00	0.00
ap	1.03	1.26	1.14	1.31	1.08	1.08	1.11	1.05	1.28	1.05
Rock type	basalt	basalt	basalt	trachy- basalt	basalt	basalt	basalt	basalt	basalt	basalt

Table 2. Continued

Map Unit	H255	PyC	PyC	UPL	UPL	PyC	ALF	ALF	CHVC
SAMPLE	9841	9845	9854	9871	9819	9852	9831	9875	9846
Q	0.00	0.00	0.00	0.00	0.00	0.00	0.00	0.00	0.00
or	5.97	5.25	10.39	7.12	8.80	10.14	9.01	9.61	8.86
ab	22.28	23.26	14.94	19.67	21.17	12.58	18.80	17.89	18.56
an	18.99	19.93	17.49	18.52	19.35	16.05	20.69	19.20	20.66
lc	0.00	0.00	0.00	0.00	0.00	0.00	0.00	0.00	0.00
ne	3.47	2.25	9.87	6.59	5.49	12.66	6.47	8.29	6.76
kal	0.00	0.00	0.00	0.00	0.00	0.00	0.00	0.00	0.00
C	0.00	0.00	0.00	0.00	0.00	0.00	0.00	0.00	0.00
di	20.84	19.84	20.85	22.04	20.30	24.05	18.66	20.26	22.48
hy	0.00	0.00	0.00	0.00	0.00	0.00	0.00	0.00	0.00
wo	0.00	0.00	0.00	0.00	0.00	0.00	0.00	0.00	0.00
ol	17.12	18.64	13.57	14.15	13.51	10.72	13.25	11.46	9.62
ac	0.00	0.00	0.00	0.00	0.00	0.00	0.00	0.00	0.00
mt	5.69	5.57	6.24	5.90	5.76	6.56	6.37	6.43	6.35
il	4.61	4.42	5.31	4.88	4.70	5.75	5.49	5.57	5.48
hem	0.00	0.00	0.00	0.00	0.00	0.00	0.00	0.00	0.00
ti	0.00	0.00	0.00	0.00	0.00	0.00	0.00	0.00	0.00
ap	1.03	0.85	1.34	1.14	0.93	1.50	1.28	1.29	1.25
Rock type*	basalt	basalt	basanite	basalt	trachy- basalt	basanite	basanite	basanite	trachy- basalt

Table 2. Continued

Map Unit	HH	CHVC	FXH	FXH	RuH	FXH	FXH	RuH	CHVC	CHVC
SAMPLE	9804	9856	SWPT 2	FXH 1	9878	SWPT 3	SWPT 1	9818	9858	9849
Q	0.00	0.00	0.00	0.00	0.00	0.00	0.00	0.00	0.00	0.00
or	6.67	9.10	10.43	10.67	14.15	10.23	10.54	13.52	9.38	9.35
ab	23.80	18.39	14.91	14.84	17.41	15.85	15.24	14.01	20.11	20.44
an	22.42	19.84	17.84	18.45	20.25	18.63	18.23	18.07	20.54	19.90
lc	0.00	0.00	0.00	0.00	0.00	0.00	0.00	0.00	0.00	0.00
ne	3.69	7.92	10.11	9.85	7.15	9.41	9.80	11.60	7.47	7.65
kal	0.00	0.00	0.00	0.00	0.00	0.00	0.00	0.00	0.00	0.00
C	0.00	0.00	0.00	0.00	0.00	0.00	0.00	0.00	0.00	0.00
di	20.26	22.21	21.36	20.76	15.92	20.78	20.86	20.13	21.23	20.98
hy	0.00	0.00	0.00	0.00	0.00	0.00	0.00	0.00	0.00	0.00
wo	0.00	0.00	0.00	0.00	0.00	0.00	0.00	0.00	0.00	0.00
ol	11.43	9.49	10.57	10.54	10.92	10.11	10.47	8.66	7.81	8.31
ac	0.00	0.00	0.00	0.00	0.00	0.00	0.00	0.00	0.00	0.00
mt	5.85	6.33	7.08	7.13	6.60	7.16	7.11	6.59	6.49	6.44
il	4.81	5.44	6.43	6.48	5.80	6.51	6.46	5.78	5.64	5.59
hem	0.00	0.00	0.00	0.00	0.00	0.00	0.00	0.00	0.00	0.00
ti	0.00	0.00	0.00	0.00	0.00	0.00	0.00	0.00	0.00	0.00
ap	1.07	1.29	1.27	1.30	1.81	1.32	1.30	1.65	1.33	1.34
Rock type'	basalt	tephrite	basanite	basanite	basalt	basanite	basanite	tephrite	tephrite	trachy- basalt

Table 2. Continued

Map Unit	RuH	CHVC	BHVC	BHVC	BHVC	BHVC	BHVC	POL
SAMPLE	9823	9857	9847	9873	9826	9872	9827	9835
Q	0.00	0.00	0.00	0.00	0.00	0.00	0.00	8.53
or	14.87	9.71	9.63	10.92	11.01	11.03	13.13	25.88
ab	14.42	20.44	20.50	20.13	19.53	20.89	21.32	41.76
an	14.64	20.40	20.48	19.75	19.57	19.51	16.65	10.95
lc	0.00	0.00	0.00	0.00	0.00	0.00	0.00	0.00
ne	14.79	7.40	7.54	8.93	9.18	9.01	7.99	0.00
kal	0.00	0.00	0.00	0.00	0.00	0.00	0.00	0.00
C	0.00	0.00	0.00	0.00	0.00	0.00	0.00	0.00
di	18.50	21.02	22.62	20.04	20.25	20.64	21.09	6.56
hy	0.00	0.00	0.00	0.00	0.00	0.00	0.00	0.64
wo	0.00	0.00	0.00	0.00	0.00	0.00	0.00	0.00
ol	7.77	7.43	5.56	5.83	5.95	4.19	2.83	0.00
ac	0.00	0.00	0.00	0.00	0.00	0.00	0.00	0.00
mt	6.86	6.53	6.58	6.82	6.85	6.96	7.80	3.50
il	6.15	5.70	5.77	6.09	6.14	6.28	7.37	1.71
hem	0.00	0.00	0.00	0.00	0.00	0.00	0.00	0.00
ti	0.00	0.00	0.00	0.00	0.00	0.00	0.00	0.00
ap	1.99	1.37	1.33	1.49	1.52	1.50	1.82	0.49
Rock type	tephrite	trachy- basalt	trachy- basalt	tephrite	tephrite	tephrite	tephrite	trachyte

Geological Map of St. Paul Island

The new map of the volcanic geology of St. Paul Island (Plate 1) covers the entire island at a scale of 1:28,000. Seventeen different volcanic units are mapped in addition to greater than 40 vents (Plate 1). Because this study has focused on the volcanic geology of St. Paul Island, thin and discontinuous coverings of eolian sediments are not illustrated on the map. Undifferentiated lavas (UPL) and (ULF) are those with source vents that are either no longer preserved or have not been located. The platform lavas (UPL) are best exposed on the southern promontories and near vicinity where they have been extensively faulted. The oldest lava flows in this unit may not be shown on the map (Plate 1) because they are exposed near sea level at the base of nearly vertical sea cliffs. Undifferentiated lava flows (ULF) are located inland and have not undergone apparent large magnitude faulting. Pyroclastic cones with no identified lava flows are grouped together in the PyC unit; this unit includes Black Bluffs, the remnant of a Surtseyan volcano. The Bogoslof Hill and Cone Hill volcanic complexes (BHVC and CHVC) are polygenetic volcanoes, and the remainder of the units (the majority) are monogenetic scoria cones and their associated lava flows. Monogenetic volcanoes are defined as volcanoes that are formed during one eruptive episode, usually lasting for less than a year, and then become extinct, while polygenetic volcanoes may erupt repeatedly from the same central vent, or group of closely spaced vents and have life spans of up to 1 Ma.

Relative and numerical dating methods were used to construct the geological column for St. Paul Island (Plate 1). Relative age determinations of units were made using a

combination of three methods: (1) stratigraphic relationships between volcanic deposits, (2), faulting, and (3) cover of sediment and vegetation on lava flows. Relative age determinations are, where possible, corroborated by radiometric dating. Petrographic and geochemical similarities were used to confirm field evidence and to correlate volcanic deposits.

Stratigraphic relationships between stacked lava flows exposed in cross-section in sea cliffs are locally obvious. Faults and fissures cut several of the volcanic units on St. Paul Island. [The term *fissure* is used to designate a fracture or crack in the rocks along which there is a distinct separation (Jackson, 1997).] On the island surface, age relationships may or may not be clear. In some areas, younger lava flows clearly cover older deposits and also flow around the bases of pyroclastic cones. Pyroclastic deposits may also cover older lava flows. Excellent examples of such stratigraphic relationships are located at the Fox Hill cinder cone and its associated lava flow (FXH) on western St. Paul Island (Plate 1). In other areas, contacts between adjacent lava flows are less clear because they are obscured by thin covers of sediment and vegetation. The thickness of eolian sedimentation and cover of vegetation on volcanic deposits was sometimes useful in distinguishing the relative ages of lava flows. Along contacts, the older flows are less well exposed, with sediments and tundra vegetation occupying the interstices between the flow-surface boulders.

Descriptions and Interpretations of Map Units

Descriptions and interpretations of the mapped units are presented below according to inferred stratigraphic order. Rock names (see Figure 4 and Table 2) and brief descriptions of petrography are included in unit descriptions. The weight percent of MgO in the rock (Table 1) distinguishes unevolved ($>10\%$) from moderately evolved (10 to 8%) from evolved ($<8\%$).

Undifferentiated Platform Lavas (UPL) Description

Undifferentiated platform lavas (UPL) are composed of multiple, often faulted, basaltic lava flows that form the base of St. Paul Island. These older lavas are more extensively faulted than the morphologically younger volcanic units emplaced upon them. Platform lavas are exposed along the wave eroded coastal cliffs where the steepness of the cliffs often precludes illustrating them on the geological map. Upland exposures occur along the southern coast and inland on south central St. Paul at Kaminista. Kaminista, an enigmatic, positive topographic area of faulted platform lava, is discussed below.

The most complete and accessible exposures of the platform lavas occur at four locations. These are (1) Reef Point, the southernmost part of the island, (2) Tolstoi Point, on southern St. Paul, (3) Zapadni Point, on the southwestern coast, and (4) Einahnuhto Bluffs, along the west coast. At these locations, vertical sections of stacked, generally horizontal, pahoehoe lava flows are exposed from sea level to the top of the volcanic pile.

Individual lava flows range in thickness from <1 m to > 20 m. They appear to be both compound and simple and are often laterally discontinuous over short distances. Ropy flow surfaces and vesicular flow tops are commonly preserved and pipe vesicles often occur in flow bases (Fig. 5, A and B). Evidence for emplacement of some platform lavas by tube flow is located at Southwest Point, where a lava tube is exposed near sea level beneath stacked lava flows (Fig. 6).

A**B**

Figure 5. Pahoehoe flow lobe details. A. Pahoehoe ropes and pipe vesicles. B. Thin flow lobes with pipe vesicles at base and vesicles in flow tops. Hammer for scale is 33 cm in length.



Figure 6. Lava tube near sea level at Southwest Point. Hammer is about 33 cm in length.

At the extremity of Reef Point, at least two lava flows are exposed in the sea cliff. The base of the lower flow is not exposed, however, the flow is at least 3 m thick and it is overlain by a second flow approximately 5 m thick. These columnar jointed lava flows appear unweathered, with well-preserved pahoehoe features of ropes and toes between flows (Fig. 7). The upper flow has pipe vesicles in its base and also closely spaced (5 to 10 cm apart), meter long, segregation or degassing structures. Reef Point flows (lower flow, SP98-09; upper flow, SP98-10) are crystal-rich and petrographically very similar to flows sampled on Tolstoi Point (SP98-14, SP98-15). Samples SP98-10 and SP98-14 are compositionally indistinguishable basalts (Table 1).

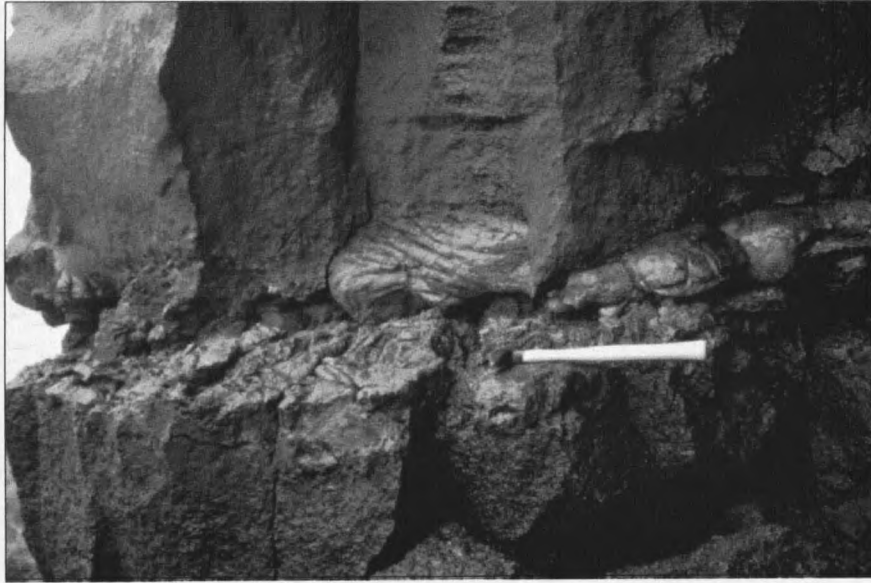


Figure 7. Lava toes and columnar jointing in lava flow lobes at Reef Point. Hammer is about 33 cm in length.

More extensive examples of the stratigraphy of the platform basalts are exposed in vertical-section in the cliffs along the south side of Tolstoi Point and on western Zapadni Point. Basalt flows on Tolstoi Point were emplaced over marine and beach sediments that are variously fossiliferous, clast-rich with well-rounded basaltic clasts, and cross-bedded with reworked tephra (Fig. 8). On southern Tolstoi Point the thickness of the early platform lava flows are estimated to be 0.5 to 15 m, with thinner flows toward the bottom and the thickest, most massive flow at the top of the section (Fig. 9). The upper flow at Tolstoi Point is a massive simple flow, about 30 m thick, with distinctive platy jointing.



Figure 8. Marine and beach sediments at Tolstoi Point.



Figure 9. Lava flows at Tolstoi Point thicken upward. Thicknesses of lava flows are indicated by bars on left side of figure. Geologist is at lower center for scale. The object in the foreground is a shipwreck.

A similar, thick (approximately 25 m), massive flow with platy jointing is exposed on the highest level of the steep southwest facing cliff at Zapadni Point (Fig. 10). Both this flow and the massive flow at Tolstoi Point are distinctive in that they have the highest proportions of modal plagioclase (41% (SP98-13) and 54% (SP98-71); see Table 1) on the island. MgO content in lavas at Zapadni Point decreases upsection, from 14 wt% in the lower flow (SP98-70) to 9.5 wt% in the upper flow (SP98-71). In the thick, platy-jointed lava flows at Tolstoi Point and Zapadni Point, the vast majority of plagioclase crystals are lath-shaped and have lengths ranging up to 1.5 mm. They are frequently

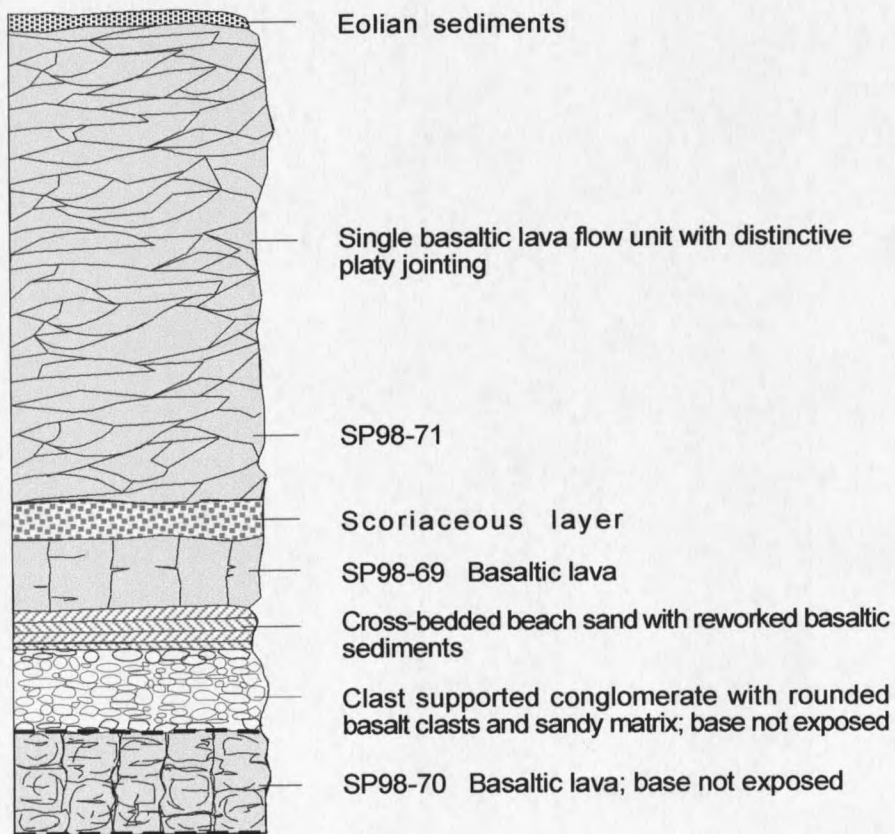


Figure 10. Schematic diagram of stratigraphy at Zapadni Point. Approximately 40 m of vertical section is exposed in west-facing cliff. Sample numbers show approximate collection sites.

aligned, giving a trachytic texture to the rock. The presence of these plagioclase laths may reflect slow, late-stage crystallization due to the thickness of the units. Although similar field appearance and petrography, the two massive units may represent separate flows because the Tolstoi Point flow (SP98-13) is slightly less evolved (10.55 wt% MgO) than the flow at Zapadni Point (SP98-71; 9.43 wt% MgO).

At Einahnuhto Bluffs the stratigraphy of the eruptive sequence is more complex than on Tolstoi Point and Zapadni Point. Among the lower units beneath Einahnuhto Bluffs is basaltic lava that appears to have intruded into wet marine sediments. Evidence for this is the presence of pillow lavas, some as great as 3 m in diameter, embedded in a brecciated matrix of quenched and hydrofractured basaltic lapilli and tuff plus sandy sediments. This unit is interpreted as a peperite formed during intrusion and quenching of basaltic magma in water-saturated sediments. Overlying this unit are compound pahoehoe lava flows similar to those described at other platform outcrops (Fig. 11). Exposed in the sea cliff beneath Rush Hill is a platy-jointed, tabular body of lava (sample SP98-18) that cuts up-section through a layer of sediments before its near-horizontal intrusion into a layer of scoriaceous lapilli-sized tephra. This lava body was also described by Barth (1956), who attributed its origin to an intrusive dike that was emplaced following the explosive eruption of Rush Hill. Lava flows at Einahnuhto Bluffs are overlain by the large and complex Rush Hill cinder cone and associated lava flows. Lava flows exposed in the cliffs at Einahnuhto Bluffs and the northern west coast generally decrease in MgO content upsection.

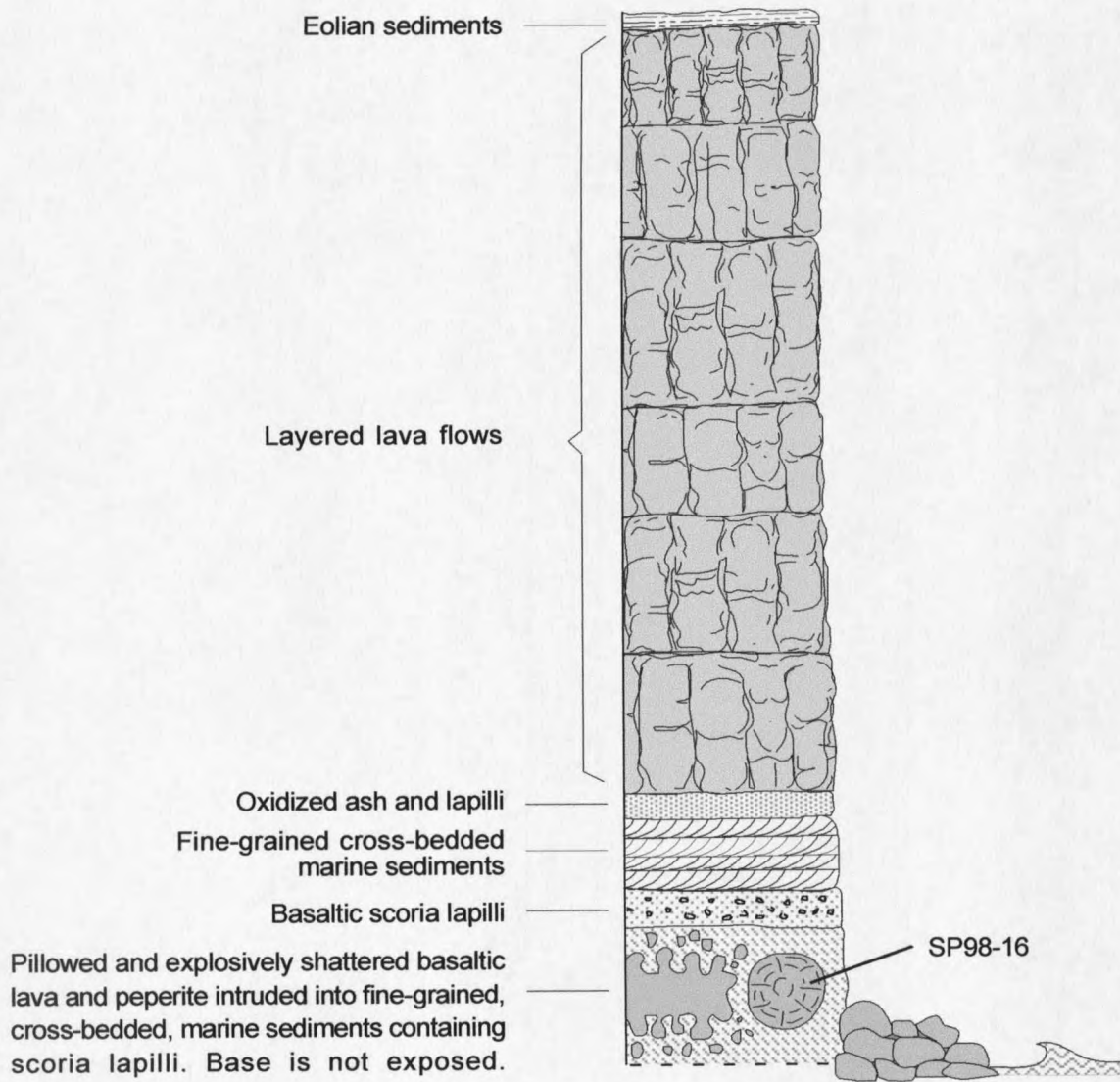


Figure 11. Schematic diagram of vertical section at Einahnuhto Bluffs on St. Paul's west coast. Height of section is about 75 m.

Locations of source vents for UPL's are unknown. On most of the island's surface there is a puzzling lack of geomorphically old cinder cones [such as those on south central and southernmost St. Paul Island, e.g., Telegraph Hill and those south of it] that may be considered as source vent for some of the platform lavas.

Platform lavas are primarily basalts and basanites, with one occurrence of trachybasalt, that range in composition from unevolved (MgO wt% >10) to moderately evolved (MgO wt% 8 to 10), although most are unevolved, and some have MgO contents as great as 14.39 wt%. Compositions of the platform lavas do not display any trends with respect to geographic position, however, MgO contents generally decrease upsection at any given locality. They all contain abundant phenocrysts of early crystallizing olivine (11 to 23 modal %) and have widely varying contents of clinopyroxene and plagioclase (0 to 24 modal % and 0 to 54 modal % respectively). Platform lavas, like many St. Paul lavas, have opaques of Fe-Ti oxides in their groundmasses, but these are usually too small to count as phenocrysts. Olivine phenocrysts in platform lavas have large variations in size and habit, from euhedral megacrysts to subhedral crystals and embayed skeletal forms. Groundmasses range from mostly glassy to intersertal and intergranular textures composed of microcrystalline plagioclase, clinopyroxene, olivine, and opaques. Some are dense and others have varying degrees of vesicularity. The most phenocryst-rich of the platform lavas are located at Kaminista and on the southern promontories. In these lavas modal olivine remains high ($\geq 14\%$) and modal clinopyroxene is variable (1 to 24%), however, modal plagioclase is remarkably high (21 to 54%). Most of the plagioclase phenocrysts occur in euhedral laths, but a few are more equant, often

subhedral, and zoned. Photomicrographs of various platform lava textures are shown in Figure 12.

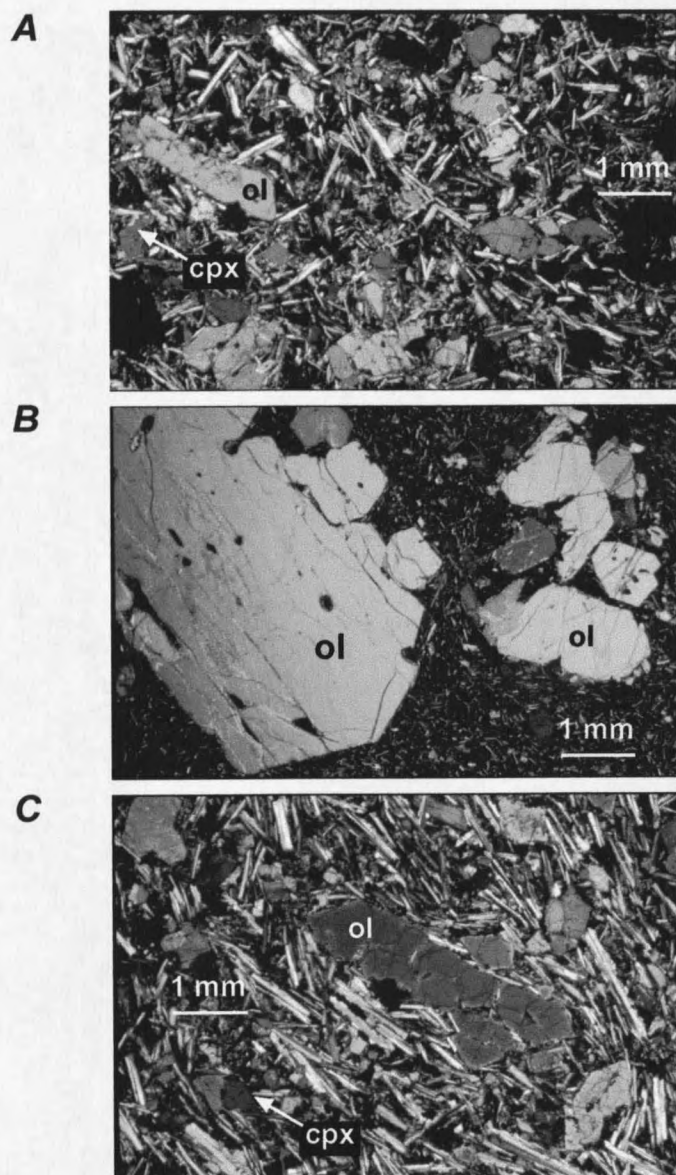


Figure 12. Photomicrographs showing textures of platform lavas. All views with crossed polars. A. Many platform lavas are characterized by their holocrystalline nature and high phenocryst content (SP98-14). B. Olivine megacrysts are common in the most MgO-rich platform lavas (SP98-70). C. Very high phenocryst contents (especially of large plagioclase laths) and trachytic texture is characteristic of lavas with platy jointing (SP98-71).

Kaminista Description. Faulted platform lavas are exposed at Kaminista, an elevated and topographically defined area located between Telegraph Hill and Bogoslof Hill. Kaminista is given special consideration here because of previous descriptions in the literature (Barth, 1956; Cox et al., 1966). Barth's (1956) brief account of Kaminista described lava flows that appeared to originate from a system of fissures. Cox et al., (1966) wrote of large fissures of probable tectonic origin in lavas at Kaminista. Kaminista is included with the platform lavas, based on composition, petrography, and faulting of the rocks. Specifically, lava at Kaminista (KAM-1) has relatively high MgO content (11 wt%) and is crystal-rich with modal plagioclase (40%), olivine (19 %), and clinopyroxene (24%). KAM-1 is petrographically and compositionally similar to UPL lava from Tolstoi Point (SP98-13).

The most prominent feature of Kaminista is a slightly curved ridge of lava that trends northeastward and southwestward; at its center it dips at 27° to 32° to the southeast (043°). Kaminista is seen from the southeast as a planar, rocky ridge (Fig. 13) that rises abruptly to 50 m above the adjacent undifferentiated lava flows (ULF). The ridge rises more steeply at the southwest end and it tapers and broadens toward the northeast (Fig. 14A). Located on this slope is a series of terrace-like features, only a few meters wide, with nearly horizontal surfaces composed of loose boulders (Fig. 14B).



Figure 13. Kaminista ridge with view to the northeast. The ridge rises abruptly from the lowland to the southeast (right). Terrace-like feature in lower left is described in text.

A curved, trench-like feature [fissure of Barth (1956) and Cox et al. (1966)] adjacent to the northwest side of the high ridge of Kaminista, separates the ridge from the topographically lower and larger expanse of the Kaminista lava field where faulting is extensive. The trench, or fissure, is a natural feature that has been minimally changed by excavations related to a quarry at its southern end (Fig. 14A) (A. Bourdukofsky, 2000, personal commun.). A low graben-like feature is located in the center of Kaminista and extensional fissures are located toward the edges (Fig. 14A).

A vertical section of the Kaminista lava pile is exposed in the quarry wall, where it is about 50 m thick and is composed of at least four flow layers or lobes (Fig 14C). Individual units of Kaminista's compound lava flow have vesicular tops with ropy surfaces and no deposits of sediment or soil between them. These lavas resemble the older platform basalts in that lower flows have columnar to blocky fracture while the top

layer has the platy fracture pattern seen at Tolstoi Point and Zapadni Point. No evidence (e.g., tephra) was found to suggest that Kaminista is a primary volcanic feature.

Kaminista Interpretation. The following interpretation is a possible scenario to explain the geologic features of Kaminista. After emplacement of old platform lavas in the Kaminista area, faulting uplifted the lava flows to a level that prevented them from being covered by younger units. Possibly, motion on orthogonal faults had combined elements of oblique dip-slip, dextral strike-slip, and extension. The oblique strike-slip motion impinged on a curved fault causing compression that uplifted and tilted the southeastern part of the Kaminista lava and shoved it into a high ridge with the original planar flow surface dipping steeply to the southeast (Fig. 14A). Stress on the planar slope opened a series of crevasses that filled with boulders and formed the terrace-like features (Fig. 14B); some oblique dip-slip motion may also have occurred along these fissures. The oblique sense of motion changed to nearly pure strike-slip on the northeast exposure of the fault where the ridge slope tapers off gently. The proposed extensional component dilated the center of the Kaminista structure, forming a graben-like feature and a series of extensional fissures or cracks on the flow surface. The trench-like feature that separates the raised southeast ridge of lava from the collapsed main body of the unit follows the main strike-slip fault trace (Fig. 14A). Fissure-like features on the northeast end of Kaminista are interpreted as splays of the strike slip fault. The direction of extension at Kaminista parallels that on Tolstoi Point, suggesting that both may be part of a larger fault system buried beneath younger lava flows on the central highland (Plate 1).

